Available on CMS information server

CMS AN -2011/258

The Compact Muon Solenoid Experiment

Analysis Note

The content of this note is intended for CMS internal use and distribution only

14 June 2011 (v5, 07 July 2011)

Search for New Physics with Same-Sign Dileptons using the 2011 dataset of CMS

D. Barge, C. Campagnari, P. Kalavase, D. Kovalskyi, V. Krutelyov, J. Ribnik

University of California, Santa Barbara

W. Andrews, G. Cerati, D. Evans, F. Golf, I. MacNeill, S. Padhi, Y. Tu, F. Würthwein, A. Yagil, J Yoo

University of California, San Diego

L. Bauerdick, I. Bloch, K. Burkett, I. Fisk, Y. Gao, O. Gutsche, B. Hooberman, S. Jindariani, J. Linacre

Fermi National Accelerator Laboratory, Batavia, Illinois

Abstract

We have repeated the 2010 same sign dilepton + jets + missing energy SUSY search documented in SUS-10-004 with the first 976 pb^{-1} of 2011 data. We find no excess beyond the standard model. We provide a prescription to use our results to set limits on physics beyond the standard model based on the generator level information.

Search for New Physics with Same-Sign Dileptons using the 2011 dataset of CMS

D. Barge, C. Campagnari, P. Kalavase, D. Kovalskyi, V. Krutelyov, J. Ribnik

University of California, Santa Barbara

W. Andrews, G. Cerati, D. Evans, F. Golf, I. MacNeill, S. Padhi, Y. Tu, F. Würthwein, A. Yagil, J Yoo

University of California, San Diego

L. Bauerdick, I. Bloch, K. Burkett, I. Fisk, Y. Gao, O. Gutsche, B. Hooberman, S. Jindariani, J. Linacre

Fermi National Accelerator Laboratory, Batavia, Illinois

Abstract

We have repeated the 2010 same sign dilepton $+$ jets $+$ missing energy SUSY search documented in SUS-10-004 with the first $976\ \mathrm{pb}^{-1}$ of 2011 data. We find no excess beyond the standard model. We provide a prescription to use our results to set limits on physics beyond the standard model based on the generator level information.

Contents

1 Introduction

In this note we describe a search for new physics in the 2011 same sign isolated dilepton sample (ee, $e\mu$, and $\mu\mu$). All standard model sources of same sign isolated dileptons for $976\ \mathrm{pb}^{-1}$ at CMS are vanishingly small. The yield in this final state is thus dominated by one isolated lepton from $t\bar{t}$, Drell Yan, or W production, and a "lepton fake". In addition, there may be same sign yield contributions from charge mis-identification, especially in the ee and $e\mu$ channel, and possibly a small contribution form multi-jet events where both leptons are fakes. Throughout this note, we refer to as "fake lepton" any lepton that is not a prompt isolated lepton from a W, Z, or some beyond the standard model source like it. In particular, electrons from conversions, muons from K/π in flight decay, electrons or muons from heavy flavor decay, etc. are all referred to as "fake leptons".

This note reproduces the published analysis SUS-10-004 with the first $976\ \mathrm{pb}^{-1}$ of 2011 data [20] with the following improvements:

- Trigger strategy for higher luminosity. We use purely leptonic triggers and di-lepton plus H_T triggers, as discussed in details in Sections 2 and 3.
- Modified lepton selections for improved fake rejection as discussed in Section 3.

Aiming for a combined analysis with other groups working on a similar search, we are applying event selections agreed for the result to be presented at the 2011 summer conferences [4].

2 Data Sets, Luminosity, and Triggers

We use the following datasets for our search:

- Data samples for the dilepton event selection are given in Table 1. These events are required to fire one of the following triggers (all trigger versions are wild-carded):
  - For the *high-p_T* analysis (both leptons with $p_T > 10$ GeV and at least one with $p_T > 20$ GeV);
    1. dielectron events should pass `HLT_Ele17_CaloIdL_CaloIsoVL_Ele8_CaloIdL_CaloIsoVL` or `HLT_Ele17_XXLstr_Ele8_XXLstr` (where `XXLstr` stands for `CaloIdT_TrkIdVL_CaloIsoVL_TrkIsoVL`);
    2. electron-muon events should pass `HLT_Mu17_Ele8_CaloIdL` or `HLT_Mu8_Ele17_CaloIdL`;
    3. dimuon events should fire `HLT_DoubleMu7` for runs up to 164236 or `HLT_Mu13_Mu8` for the following runs.
  - For the *low-p_T* analysis (selections with muons $p_T > 5$ GeV or electrons $p_T > 10$ GeV);
    1. dielectron events should pass `HLT_DoubleEle8_CaloIdL_TrkIdVL_HT160` or `HLT_DoubleEle8_CaloIdT_TrkIdVL_HT160` up to run 163261; `HLT_DoubleEle8_CaloIdL_TrkIdVL_HT150` or `HLT_DoubleEle8_CaloIdT_TrkIdVL_HT150` for runs from 163269;
    2. electron-muon events should pass `HLT_Mu3_Ele8_CaloIdL_TrkIdVL_HT160` or `HLT_Mu3_Ele8_CaloIdT_TrkIdVL_HT160` up to run 163261; `HLT_Mu3_Ele8_CaloIdL_TrkIdVL_HT150` or `HLT_Mu3_Ele8_CaloIdT_TrkIdVL_HT150` for runs from 163269;
    3. dimuon events should fire `HLT_DoubleMu3_HT200` in the full run range or `HLT_DoubleMu3_HT160` up to run 163261, or `HLT_DoubleMu3_HT150` for runs from 163269.
- Datasets for fake rate measurement include datasets culled on single-lepton triggers (with an additional jet sometimes) are listed in Table 2. Note that single lepton triggers are required in this case (see details later) as following:
  - Electron fake rates are measured in events passing one of the following triggers (all selected in the `/DoubleElectron` primary datasets)
    1. `HLT_Ele8`,

2. or HLT_Ele8_CaloIdL_CaloIsoVL,
3. or HLT_Ele8_CaloIdL_CaloIsoVL_Jet40,
4. or HLT_Ele17_CaloIdL_CaloIsoVL;

– Muon fake rates are measured in events passing one of the following triggers (all triggers are in the /SingleMu primary dataset, except for HLT_Mu8_Jet40, which is taken from the /DoubleMu)

1. HLT_Mu5,
2. or HLT_Mu8,
3. or HLT_Mu8_Jet40,
4. or HLT_Mu12,
5. or HLT_Mu30.

- Monte Carlo samples used for the estimates of the dilepton event yields are summarized in Table 3. These samples are produced as part of the Spring11 MC campaign. We plan to move to Summer11 samples once all are available.

- MC samples used for closure tests of fake rates are provided in Table 4.

Name	Run Range
/DoubleElectron/Run2011A-May10ReReco-v1/AOD	160329-163869
/DoubleElectron/Run2011A-PromptReco-v4/AOD	165071-167784
/DoubleMu/Run2011A-May10ReReco-v1/AOD	160329-163869
/DoubleMu/Run2011A-PromptReco-v4/AOD	165071-167784
/MuEG/Run2011A-May10ReReco-v1/AOD	160329-163869
/MuEG/Run2011A-PromptReco-v4/AOD	165071-167784
/ElectronHad/Run2011A-May10ReReco-v1/AOD	160329-163869
/ElectronHad/Run2011A-PromptReco-v4/AOD	165071-167784
/MuHad/Run2011A-May10ReReco-v1/AOD	160329-163869
/MuHad/Run2011A-PromptReco-v4/AOD	165071-167784

Table 1: Signal analysis datasets. Note that the events are considered in the order of the datasets as shown below. If an event has already appeared in a previous dataset, it is skipped. The last run in the PromptReco-v4 datasets corresponds to the last good run certified on June 3, 2011.

Name	Run Range
/DoubleElectron/Run2011A-May10ReReco-v1/AOD	160329-163869
/DoubleMu/Run2011A-May10ReReco-v1/AOD	160329-163869
/SingleMu/Run2011A-May10ReReco-v1/AOD	160329-163869
/DoubleElectron/Run2011A-PromptReco-v4/AOD	165071-167151
/DoubleMu/Run2011A-PromptReco-v4/AOD	165071-167151
/SingleMu/Run2011A-PromptReco-v4/AOD	165071-167151

Table 2: Datasets for fake rate measurement include datasets culled on single-lepton triggers (with an additional jet sometimes). Note that single lepton triggers contributing to the given PD are required in this case (see details later).

For the dilepton data analysis we use a combination of good run lists (JSON files) certified for May10ReReco datasets (runs 160404-163869) and for PromptReco datasets certified on July 1 (runs 165071 to 167784). This list of certified good runs corresponds to an integrated luminosity of 976 pb^{-1}.

The fake rates are currently measured on a smaller data sample. The electron fake rates are measured using the May10ReReco dataset and a corresponding good run list. The measurement of the muon fake rates is done using the PromptReco datasets and a corresponding list of good runs from May 6 (there are no significant differences expected for muons, unlike in the case for electrons). For both the muon and electron fake rates the data sample corresponds to approximately 140 pb^{-1}. We do not expect any dependence of the fake rates as a function of time and currently use a reduced dataset due to limited CPU/time resources.

Name	Cross section, pb
TTJets_TuneZ2_7TeV-madgraph-tauola_Sp11-v1	157.5
TToBLNu_TuneZ2_tW-channel_7TeV-madgraph_Sp11-v1	10.6
TToBLNu_TuneZ2_t-channel_7TeV-madgraph_Sp11-v1	20.9
TToBLNu_TuneZ2_s-channel_7TeV-madgraph_Sp11-v1	1.4
WJetsToLNu_TuneZ2_7TeV-madgraph-tauola_Sp11-v1	31314
DYJetsToLL_TuneD6T_M-50_7TeV-madgraph-tauola_Sp11-v1 gen Z mass $>$ 50 GeV	3048
DYToEE_M-20_CT10_TuneZ2_7TeV-powheg-pythia_Sp11-v1 gen Z mass 20—50 GeV	1666
DYToMuMu_M-20_CT10_TuneZ2_7TeV-powheg-pythia_Sp11-v1 gen Z mass 20—50 GeV	1666
DYToTauTau_M-20_CT10_TuneZ2_7TeV-powheg-pythia-tauola_Sp11-v1 gen Z mass 20—50 GeV	1666
DYToEE_M-10To20_TuneZ2_7TeV-pythia6_Sp11-v1	3892.9
DYToMuMu_M-10To20_TuneZ2_7TeV-pythia6_Sp11-v1	3892.9
DYToTauTau_M-10To20_CT10_TuneZ2_7TeV-powheg-pythia-tauola_Sp11-v2	3892.9
WWTo2L2Nu_TuneZ2_7TeV-pythia6_Sp11-v1	4.5
WZtoAnything_TuneZ2_7TeV-pythia6-tauola_Sp11-v1	18.2
ZZtoAnything_TuneZ2_7TeV-pythia6-tauola_Sp11-v1	5.9
PhotonVJets_7TeV-madgraph_Sp11-v1	173
PhysicsProcesses_doublePartonWWFastSim	0.378
PhysicsProcesses_WplusWplus	0.165
PhysicsProcesses_WminusWminus	0.055
PhysicsProcesses_ttbarW (non-top W is $W \to \ell\nu$)	0.079
LM6_SUSY_sftsht_7TeV-pythia6_Sp11-v1	0.31 (LO)
LMXXX_SUSY_sftsht_7TeV-pythia6_Sp11-v1, all are available	

Table 3: MC datasets. The common part of each dataset name Spring11-PU_S1_START311_V1G1 is replaced with a shorthand Sp11. All datasets are in the AODSIM data tier. We combine all of the Drell-Yan samples shown above to get a continuous coverage with the best available samples from 10 GeV to ∞. The datasets with PhysicsProcess in the name are generated in CMSSW_4_2 using fast simulation package.

Name	Cross section, pb	Luminosity, pb^{-1}
/QCD_Pt_30to50_TuneZ2_7TeV_pythia6_Sp11	5.31×10^7	0.12
/QCD_Pt_50to80_TuneZ2_7TeV_pythia6_Sp11	6.36×10^6	0.68
/QCD_Pt_80to120_TuneZ2_7TeV_pythia6_Sp11	7.8×10^5	6.6
/QCD_TuneD6T_HT-100To250_7TeV-madgraph_Sp11	7×10^6	0.17
/QCD_Pt-20to30_MuPt5Enriched_TuneZ2_7TeV-pythia6_Sp11	2.38×10^8	9.1
/QCD_Pt-30to50_MuPt5Enriched_TuneZ2_7TeV-pythia6_Sp11	5.31×10^7	14
/QCD_Pt-50to80_MuPt5Enriched_TuneZ2_7TeV-pythia6_Sp11	6.35×10^6	74
/QCD_Pt-80to120_MuPt5Enriched_TuneZ2_7TeV-pythia6_Sp11	7.85×10^5	109
/QCD_Pt-20_MuEnrichedPt15_TuneZ2_7TeV-pythia6_Sp11	2.97×10^8	302
TTToLNu2Q2B_7TeV-powheg-pythia6_Sp11-v1	65.8	73×10^3
WJetsToLNu_TuneZ2_7TeV-madgraph-tauola_Sp11-v1	31314	483

Table 4: MC datasets. The common part of each dataset name `Spring11-PU_S1_START311_V1G1-v1` is replaced with a shorthand `Sp11`. All datasets are in the AODSIM data tier. The `MuEnriched` samples are used to extract the muon fake rates (MuPt5 samples are used up to 15 GeV, after which the Pt15 takes over); the electron fake rates are extracted from the QCD samples.

3 Event Selection

Lepton, jet, $\not\!\!E_T$, and other event selections are based on [4].

3.1 Dilepton-H_T regions

We select events with two same sign isolated leptons (ee, $e\mu$, or $\mu\mu$). We extend the momentum phase space of the previous analysis and add a dilepton selection with lower lepton momenta:

- *high-p_T* dilepton selections require one of the leptons to have $p_T > 20$ GeV, and the other to have $p_T > 10$ GeV. This selection is inspired by the $t\bar{t}$ analysis.
- *low-p_T inclusive* dilepton selections require the two leptons with $p_T > 5$ GeV for muons and $p_T > 10$ GeV for electrons. These dileptons are only available in data from the `HT150/160` triggers, which are fully efficient with $H_T > 200$ GeV, where H_T is calculated as a sum of momenta of jets with $p_T > 40$ GeV, as described in more detail later in this section.

This is the selection chosen for the main results of the combined analysis [4].

3.2 Trigger selection

No trigger selection is applied on Monte Carlo events. The events in data are required to fire one of the triggers as described in Section 2. As discussed in Section 4, a trigger efficiency weight is applied to each event, based on the trigger efficiencies measured on data.

3.3 Event cleanup and vertex selection

- Scraping cut: if there are ≥ 10 tracks, require at least 25% of them to be high purity.
- Require at least one good primary vertex (PV), and use the first such vertex found as a reference points for further selections
  - use deterministic annealing (DA) vertices; these are the default/standard vertices in CMSSW_4_2 (data) samples, DA vertices should be selected separately in the CMSSW_4_1 (Spring11 MC) samples;
  - not fake,
  - ndof > 4,
  - $|\rho| < 2$ cm,
  - $|z| < 24$ cm.

3.4 Muon requirements

Muon candidates are RECO muon objects passing the following requirements:

- $p_T > 10$ GeV or > 5 GeV depending on the choice of dilepton momenta kinematic regions;
- $|\eta| < 2.4$;
- have both global muon and tracker muon types;
- χ^2/ndof of global fit < 10;
- at least 11 hits in the tracker fit;
- the global fit has to include at least one valid hit in the muon subdetectors;
- the relative uncertainty of muons p_T shoule be less than 0.1;
- transverse impact parameter of the silicon (inner) track with respect to the selected PV to be < 200 μm;
- the inner track z should be within 1 cm from the selected PV;

- $Iso \equiv E_T^{\rm iso}/p_T < 0.15$, where $E_T^{\rm iso}$ is defined as the sum of transverse energy/momentum deposits in ECAL, HCAL, and tracker, in a ΔR cone of 0.3, excluding the contribution from the muon itself;
- ECAL veto deposit < 4 GeV (veto deposit corresponds to the sum of E_T in the region of the calorimeter associated with the muon impact and excluded from the $E_T^{\rm iso}$);
- HCAL veto deposit < 6 GeV.

3.5 Electron requirements

Electron candidates are RECO GSF electrons passing the following requirements:

- the electron must be ecal seeded;
- $p_T > 10$ GeV;
- $|\eta| < 2.4$;
- electrons have to have $\Delta R > 0.1$ with respect to any tracker or global muon if any are present in the event;
- VBTF80 identification[6] with the cut on H/E not applied in the EE, similar to the choice made in the Higgs WW analysis [11];
- If the $p_T < 20$ GeV, the electron has to have $f_{\rm brem} > 0.15$, or to have the super-cluster $|\eta_{\rm SC}| < 1$ with $E/P > 0.95$ as used in [11];
- transverse impact parameter of the GSF track with respect to the selected PV to be $< 200\ \mu$m;
- the z coordinate of the GSF track should be within 1 cm with respect to that of the selected PV;
- the number of missing expected inner hits must be zero [8];
- electrons from photon conversions are rejected if there is a CTF partner track found with the minimal distance between the electron and the partner track in the transverse plane $|dist| < 0.02$ cm and with a difference in $\cot\theta$ of $|d_{\rm cot}| < 0.02$;
- require that all three charge measurements for a GSF electron agree; one from the charge of the GSF track, one from the charge of the CTF track associated to the GSF track and one, the so-called "supercluster charge", determined from the relative position of the supercluster with respect to the projected track from the pixel seed;
- $Iso \equiv E_T^{\rm iso}/p_T < 0.15$, where $E_T^{\rm iso}$ is defined as the sum of transverse energy/momentum deposits in ECAL, HCAL, and tracker, in a cone of 0.3; a 1 GeV pedestal is subtracted from the ecal energy deposition in the barrel (EB), however the ecal energy is never allowed to go negative;

3.6 Invariant mass requirement

We remove dilepton events with invariant mass $M_{\ell\ell} < 5$ GeV.

We veto events for which a third lepton is found that passes all the lepton requirements and makes an opposite sign same flavor Z candidate with one of the two same sign leptons we require. The Z candidate for this veto needs to have a dilepton mass within $76 - 106$ GeV.

3.7 Lepton pair disambiguation

In events with multiple lepton pairs passing the selections described above only one pair is selected following the prescription:

- the $\mu\mu$ is chosen over $e\mu$, which is chosen over ee;
- a pair with the highest sum of p_T is selected among the pairs of the same dilepton final state.

3.8 Jet and $\not\!\!E_T$ Selections

There must be two or more particle flow jets corrected with L1FastJetL2L3 (FastJet-based offset correction followed by L2 and L3 corrections) with $p_T > 40$ GeV and $|\eta| < 2.5$. The selected jets must pass loose `pfJetId` and be separated by $\Delta R > 0.4$ from any lepton passing the selection described above.

The sum of p_T of these jets defines $H_T \equiv \sum p_T^{\rm jet}$. This variable is used to define the signal event selections.

The particle flow $\not\!\!E_T$ should be $\not\!\!E_T > 30$ GeV.

4 Trigger efficiency

We rely on two types of triggers, as described in the previous sections: a) dilepton triggers without an additional jet requirement; b) dilepton triggers with an additional requirement on H_T. The trigger efficiency values are only relevant for the estimates of the signal selection efficiency.

Reference [11] discusses trigger efficiency measurements for the electron and muon triggers in considerable detail. The lepton trigger efficiencies (per lepton) are measured there relative to essentially the same lepton selections, which allows to apply these results here. We thus only summarize the values of the trigger efficiencies here. Note that these measurements were performed with the May10ReReco datasets.

The electron `CaloIdL_CaloIsoVL` triggers are measured to be approximately 99% efficient per electron over the entire η and p_T ranges relevant to this analysis with values slightly below 99% for momenta below 20 GeV$/c$. We assign an efficiency of $99 \pm 1\%$ ($99 \pm 2\%$) for $p_T > 20$ GeV$/c$ ($p_T < 20$ GeV$/c$, using symmetric uncertainty). This applies both to the electron trigger leg with and without a level-1 seed requirement. In the recent data (not yet relevant for the dataset with 350 $\rm pb^{-1}$), several of the triggers are now requiring `CaloIdT`. There is no significant inefficiency expected from this part of the trigger requirement compared to that of `CaloIdL` used now. We will thus use the same efficiency value for the triggers with `CaloIdT`.

We consider the efficiency measurement done in [11] for the `CaloIdVT_CaloIsoT_TrkIdT_TrkIsoT` to be applicable to the `CaloIdL_TrackIdVL` as well ass the `CaloIdT_TrackIdVL` trigger primitives used in the H_T triggers and assing an efficiency of $98 \pm 2\%$ per electron for this trigger. This is confirmed directly in Z events with $H_T > 200$ GeV, where we find $96.7 \pm 0.7\%$ dielectrons passing the `Ele17...Ele8` trigger with `CaloIdL_CaloIsoVL` to also pass the `DoubleEle8_CaloIdL_TrkIdVL`. Assuming the electron efficiencies factorize and there is no extra inefficiency from the H_T requirement, this conditional per-electron efficiency is $98.3 \pm 0.3\%$, in agreement with the choice of $98 \pm 2\%$ made based on the results from [11]. While there is not sufficient amount of data to confirm that this efficiency stays this high for electron momenta below 20 GeV$/c$, we take a safer approach and use a value with a larger uncertainty $98 \pm 3\%$ for $p_T < 20$ GeV$/c$. Note that the test using H_T triggers may be biased by the amount of the ignored inefficiency in the H_T trigger requirement, as discussed below. The assigned uncertainty covers this bias.

The muon trigger efficiencies measured in reference [11] are provided for muons with $p_T > 10$ GeV$/c$. The average efficiency for a trigger with an HLT requirement of $p_T > 7$ GeV$/c$ and the level-1 requirement for a 3 GeV$/c$ muon is found to be in the range of 95–97%. This measurement is expected to be an underestimate by approximately 1–2% for muons collected with the level-1 requirement of a 0 GeV$/c$ muon used in the H_T triggers with an HLT requirement of 3 GeVfor muons. Note that the electron-muon triggers without H_T requirement use an even less restrictive level-1 muon seed, open-muon seed, which has a 1–2% higher efficiency than that of the `SingleMu3` or `Mu0` seed. We simplify these results and assign an efficiency of $96 \pm 2\%$ ($90 \pm 5\%$) per muon for $p_T > 10$ GeV$/c$ ($5 < p_T < 10$ GeV$/c$), where for the low-p_T part we rely on results reported in Ref. [3].

The triggers with the H_T requirement have an additional inefficiency for this requirement. The H_T trigger turn-on curves are shown in Figures 1 and 2, both made with the first 150 $\rm pb^{-1}$ of data. For each of these trigger turn on curves, we choose a muon trigger for the denominator, and a corresponding muon plus H_T trigger for the numerator. Muons are chosen to show the worst case for the H_T-based trigger. The trigger requires the sum of the calorimeter-jet momenta with $p_T > 40$ GeV$/c$ to be above a given threshold (160, 150, or 200 GeV). While the high-p_T electrons will naturally contribute to the H_T computed in HLT, muons, being MIPs, will not. Figure 1 shows dimuon events with $p_T > 20$ GeV$/c$ and 10 GeV$/c$ respectively with a dimuon mass of at least 40 GeV$/c^2$. The muons are required to pass all of our muon selections. The denominator trigger is DoubleMu7 while the numerator is the logical `OR` of the `DoubleMu3_HT150` and `HT160` triggers. The three curves shown depict different jet selections to define H_T. The precision of this measurement is limited by the number of dimuon events with a high value of H_T. We perform a higher precision measurement using single-muon events, albeit for the only available single-muon trigger with a requirement of $H_T > 200$ GeV. Figure 2 compares HT200 turn on curves for single and double muon selections. For the single muon selection we require $p_T > 30$ GeV, deliberately veto events with a second muon with $p_T > 15$ GeV, and require the .or. of Mu8,12,30 trigger in the denominator. The numerator has the same selection except requiring as trigger `HLT_Mu8_HT200`. The double muon selection for Figure 2 is the same as in Figure 1. We count only jets in H_T that are at least $\Delta R > 0.4$ away from the muons, have $p_T > 30$ GeV, and $|\eta| < 2.5$. The agreement between the two curves increases confidence in the less precise measurement shown in Fig. 1.

Based on the observed turn-on curves, we assign an efficiency for the HT150/160 trigger to be $95 \pm 5\%$ for H_T in the range of 200–300 GeV, and $99 \pm 1\%$ for $H_T > 300$ GeV. We do not use the HT triggers for events reconstructed with $H_T < 200$ GeV.

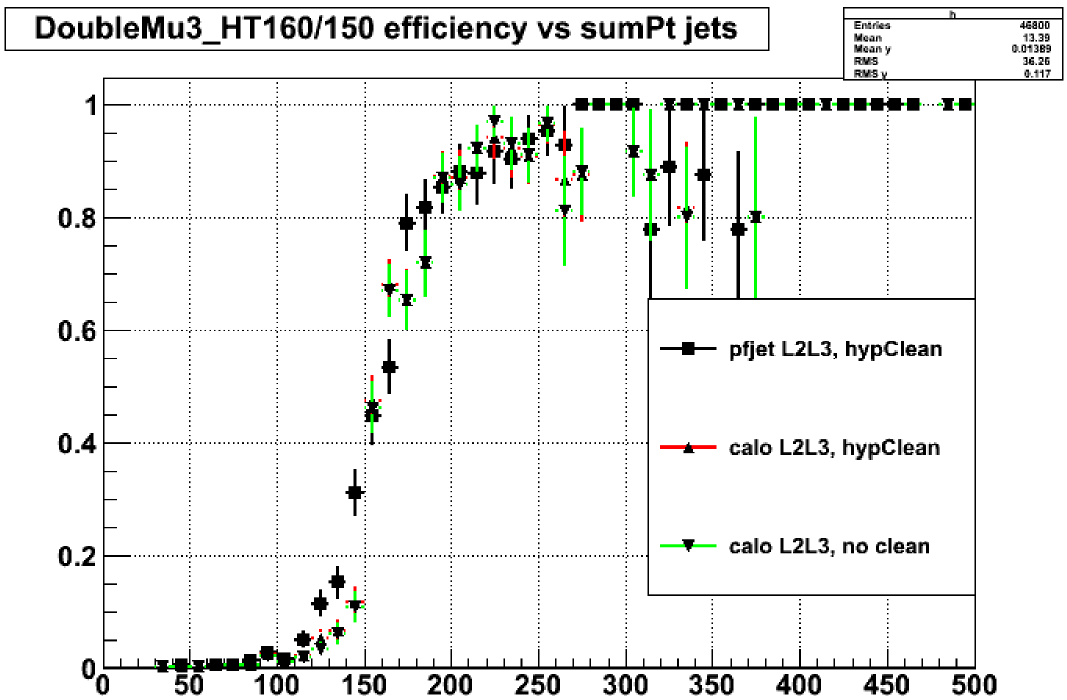

Figure 1: H_T trigger turn-on curve for the HT150/160 triggers measured using dimuon events near the Z mass. The distributions are shown as a function of H_T computed using L2L3-corrected particle-flow jets not overlapping with either of the muons (box), L2L3-corrected calorimeter jets not overlapping with either of the muons (up triangles), and L2L3-corrected calorimeter jets allowed to overlap with the two muons. In all cases the jets used are with $p_T > 30$ GeV$/c$ and $|\eta| < 2.5$.

5 Selection Efficiency

We would like to quote our results as a cross section, or cross section limit, that is as model independent as possible. What we mean by this is that we carefully define the acceptance, and provide enough details about the selection efficiency within that acceptance that anybody can use their favorite Monte Carlo generator of new physics, define an acceptance at the hard scatter level (status = 3 in Pythia), and correctly estimate the efficiency for this new physics model to within 50% or so.

In the present section we provide the necessary *correction factors* that one needs to estimate the efficiency. There are three effects. First, our lepton selection efficiencies vary significantly as a function of both p_T and $|\eta|$, especially for electrons. Second, both $\not\!\!E_T$ and H_T have *turn-on* curves due to finite resolution effects. Third, there is a small p_T dependent data/Monte Carlo scale factor that we obtain from Z to dilepton events using the tag & probe technique. Even though the scale factors are described last, we include them in the lepton efficiency parameterization presented below in Section 5.2.

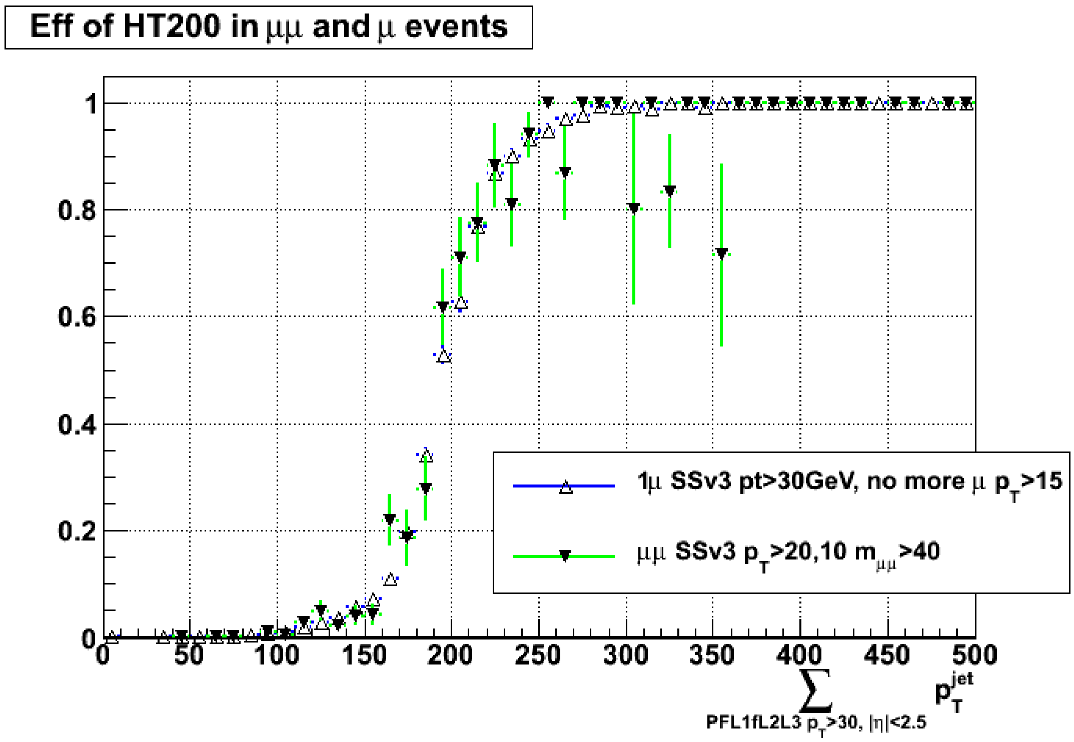

Figure 2: H_T trigger turn-on curve for the HT150/160 triggers as a function of the L1FastL2L3-corrected particle flow jets. The jets used are with $p_T > 30$ GeV$/c$ and $|\eta| < 2.5$. The curve measured for the single-muon H_T trigger in events with only one muon (open up triangles) representes the efficiency in W+jet events. The curve measured for the dimuon H_T trigger in events with two muons (down triangles) represents the efficiency in Z+jet events.

5.1 Definition of Acceptance

Lepton acceptance is defined for both leptons with $|\eta| < 2.4$ and with momenta either $p_T > 10$ GeV$/c$ (5 GeV$/c$) for electrons (muons) and the *low-*p_T dilepton selections, or with one lepton with $p_T > 10$ GeV and the other with $p_T > 20$ GeV for the *high-*p_T selections described in Section 3. $H_T^{\rm gen}$ is comprised of the sum p_T of all colored particles at the hard scatter level that have $p_T > 40$ GeV and $|\eta| < 2.5$. $\not\!\!E_T^{\rm gen}$ is defined as the absolute value of the vector sum of the transverse momentum of all non-interacting particles, e.g. neutrinos and LSP.

5.2 Lepton Efficiencies

These curves are to be taken directly from simulation, they are primarily relevant for the outside-CMS theorists to be able to use our results. A similar set of curves has been provided in [20]. Lepton selection efficiencies, including the MC-to-data scale factors, are illustrated in Fig. 3.

The efficiency dependence can be parameterzied as a function of p_T as

$$\epsilon = \epsilon_\infty \mathrm{erf}\left(\frac{p_T - C}{\sigma}\right) + \epsilon_C \left(1. - \mathrm{erf}\left(\frac{p_T - C}{\sigma}\right)\right), \tag{1}$$

where ϵ_∞ gives the value of efficiency plateau at high momenta, C is equal to 5 (10) for muons (electrons), ϵ_C gives the value of the efficiency at $p_T = C$, and σ describes how fast the transition region is. The results of the fit for electrons and muons are summarized in Table 5.

5.3 MET and H_T efficiency turn-on

Our selections on reconstructed jets begin with a requirement of at least two jets with $p_T > 40$ GeV. Two such jets are present in approximately 95% of the events in LM1 and LM6 with $H_T^{\rm gen} > 200$ GeV prior to any

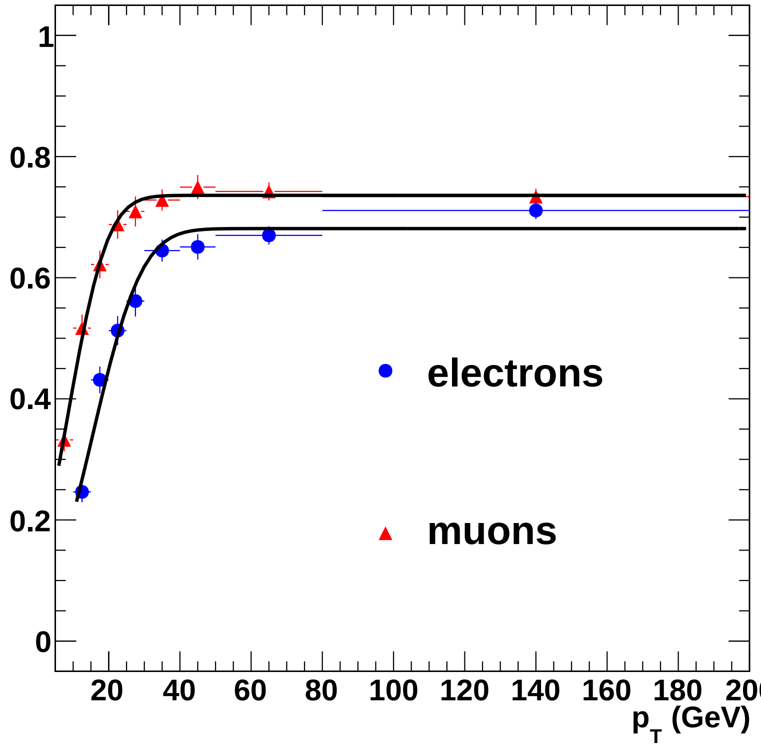

Figure 3: Lepton selection efficiency as a function of p_T, displayed for electrons and muons.

Table 5: Results of the fit of the dependence in Fig. 3 to the function specified in Eq. 1.

Parameter	Electrons	Muons
C	10	5
ϵ_∞	0.683 ± 0.010	0.736 ± 0.008
ϵ_C	0.186 ± 0.024	0.242 ± 0.029
σ	19.1 ± 1.8	14.7 ± 1.4

additional requirement on colored partons at the generator level beyond the sum of p_T. This represents the fraction of acceptance to two jets. In the following we proceed with determining H_T amd $\not{E}_T$ requirement with respect to events that have generator-level requirements on the leptons and colored particles as described in Section 5.1.

The efficiency for an event to pass a given reconstructed $\not{E}_T$ (H_T) threshold is shown in Fig. 4 as a function of $\not{E}_T^{\rm gen}$ ($H_T^{\rm gen}$) in events passing $H_T^{\rm gen} > 200$ GeV ($\not{E}_T^{\rm gen} > 30$ GeV). Due to rather small fraction of events in LM6 simulation having low H_T activity, the H_T curves are made with LM1. Results of the fits of these curves to $0.5\epsilon_\infty\{{\rm erf}[(x - x_{1/2})/\sigma] + 1\}$ are summarized in Table 6. Neither the $\not{E}_T$ nor H_T curves show a significant bias in the position of the point with half the plateau efficiency ($x_{1/2}$). The inefficiency at the plateau is essentially negligible. The width of the threshold σ increases with the value of the cut.

Table 6: Results of the fit of the dependence in Fig. 4 to $0.5\epsilon_\infty\{{\rm erf}[(x - x_{1/2})/\sigma] + 1\}$.

Parameter	H_T		$\not{E}_T$		
	> 200 GeV	> 400 GeV	> 50 GeV	> 100 GeV	> 120 GeV
ϵ_∞	0.998 ± 0.001	0.987 ± 0.002	0.998 ± 0.001	0.997 ± 0.001	0.999 ± 0.001
$x_{1/2}$	193.0 ± 4.5	378.6 ± 3.1	45.9 ± 1.2	100.2 ± 0.8	121.2 ± 0.8
σ	87.4 ± 5.9	113.2 ± 4.9	32.6 ± 1.9	37.3 ± 1.3	40.2 ± 1.3

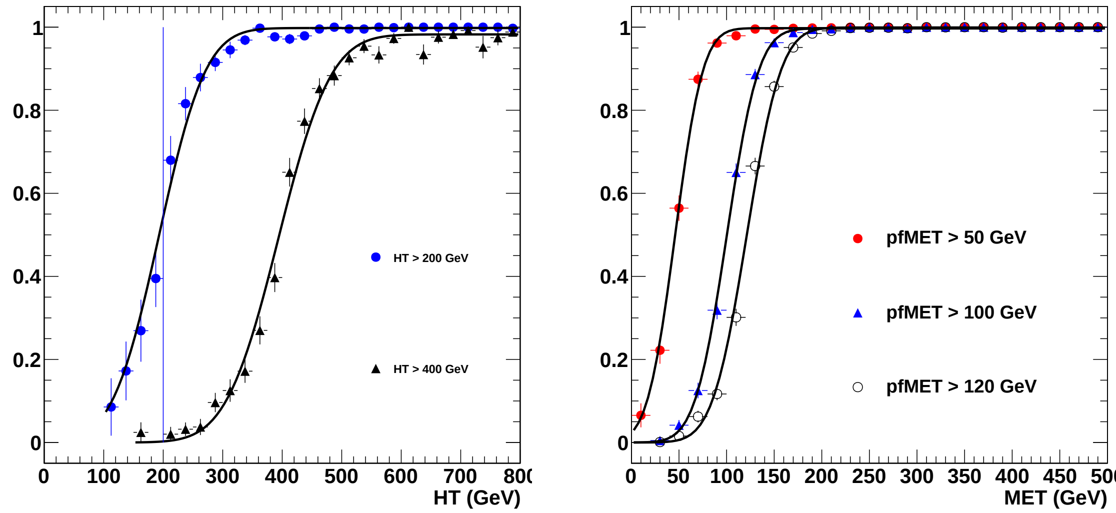

Figure 4: Efficiency for an event to pass a given reconstructed $\not\!\!E_T$ (H_T) threshold as a function of $\not\!\!E_T^{\mathrm{gen}}$ (H_T^{gen}). The curves are shown for $\not\!\!E_T$ thresholds of 50, 100, 120 GeV; the thresholds for H_T are 200, and 400 GeV.

5.4 Data - Monte Carlo Scale Factor

The efficiencies of the lepton isolation and identification (including all quality requirements) requirements are measured with the tag&probe method in dilepton Z events. The efficiency of the identification requirements is a property of the lepton itself and is directly applicable to the leptons in signal events. The efficiency of the isolation requirement, however, is a strong function of all other (mainly hadronic) activity in the event. The following results are based on the measurements in the May10ReReco datasets.

The electron selection efficiencies are measured in events passing the `Ele17..._SC8_Mass30` trigger, which requires one well-identified electron and one super-cluster with $p_T > 8$ GeV forming a pair with a mass above 30 GeV$/c^2$. In the tag&probe analysis the electron tag is required to match to the well-identified electron from the trigger and also to pass all the electron requirements described in Section 3. The probe electron is required to have

- super-cluster $E_T > 8$ GeV, $p_T > 10$ GeV, $|\eta| < 2.4$, excluding the superclusters with $1.4442 < |\eta| < 1.566$.

The isolation efficiency is measured with the probes passing all electron selections described in Section 3, except for the trigger requirement and the isolation itself. In order to reduce a bias arising from backgrounds in the electron identification efficiency measurement, we separate this measurement into four components: identification requirement proper, impact parameter selection, conversion rejection, and the triple charge requirement. Each of these four components is measured using probes failing only the requirement for which the efficiency is measured. Results of the measurement are summarized in Table 7. The contribution from the Z events is based on simple counting in the mass range of 76–106 GeV$/c$. These results are then compared with those obtained by counting events after a subtraction of the same-sign dielectron contribution, which should represent the number of backgrounds reasonably well. The effect of the background contribution to the measurement presented in Table 7 can be interpreted as a systematic uncertainty on the measurement. The size of the effect is established to be approximately 3%, 2%, and 1% for the identification efficiency for $p_T < 15$ GeV, in the 15–20 GeV$/c$ range, and above 20 GeV$/c$, respectively. The same for the isolation efficiency gives 3%, 1%, and les than 0.5% for the same momentum ranges. Based on simulation alone, the combined selection efficiency, measured with respect to the probe electron, differs from the product of the components by approximately 3%, 2%, 1%, and less than 0.3% in the momentum ranges as given in Table 7. All of these effects combined give a systematic uncertainty on the total data-to-MC scale factor in the lepton selection efficiencies of 5%, 3%, 1.5%, and 1.3%, corresponding to the momentum ranges of the Table 7.

The muon selection efficiencies are measured using events passing the double-muon trigger. The tag muon is required to pass all of the muon selection requirements described in Section 3. The probe muon is required to pass

- $p_T > 5$ GeV$/c$;

Type	source	Electron p_T range			
		10–15 GeV/c	15–20 GeV/c	20–40 GeV/c	above 40 GeV
iso	mc	0.914±0.013	0.930±0.007	0.976±0.001	0.9954±0.0003
	data	0.870±0.016	0.908±0.008	0.972±0.001	0.9938±0.0004
	data/mc	0.952±0.022	0.977±0.011	0.997±0.001	0.9984±0.0005
id	mc	0.519±0.018	0.645±0.010	0.808±0.002	0.861±0.002
	data	0.429±0.016	0.596±0.010	0.789±0.002	0.839±0.002
	data/mc	0.827±0.042	0.924±0.022	0.976±0.003	0.974±0.002
id x iso	mc	0.474±0.018	0.599±0.011	0.788±0.002	0.857±0.002
	data	0.373±0.016	0.541±0.010	0.767±0.002	0.834±0.002
	data/mc	0.787±0.044	0.903±0.023	0.973±0.003	0.972±0.002

Table 7: Electron isolation and identification efficiencies measured with the tag&probe method. The uncertainties are statistical only.

- $|\eta| < 2.4$;
- have both the global and the tracker muon types.

Both the isolation and the identification efficiency are measured using probes failing only the requirement in question, assuming the efficiencies factorize. Results of the muon identification and isolation efficiency measurements are presented in Table 8. As expected, the identification efficiency for muons measured in data and in MC agree well. Most of the reconstructed (probe) muons are real muons and the measurement of the identification efficiency is not affected significantly by backgrounds. The isolation component of the efficiency for muons below 15 GeV/c has a significant effect from backgrounds, which we estimate to be about 5%, which is treated as the systematic uncertainty. We assign a systematic uncertainty of 1% on the identification and isolation efficiency measurement for momenta above 15 GeV/c, based on the estimates of the background contribution (using same-sign pairs), and a comparison between the simple counting of Z events and fitting the mass shape to a gaussian signal and an exponential background component. Based on studies in MC events, we find that the isolation and the identification efficiencies factorize near-perfectly and do not assign any additional systematic uncertainty. The total systematic uncertainty on the muon efficiency measurement in data is 1% for momenta above 15 GeV/c, and 5% for all lower momenta.

Type	source	Muon p_T range				
		5–10 GeV/c	10–15 GeV/c	15–20 GeV/c	20–40 GeV/c	above 40 GeV/c
iso	mc	0.7532±0.0858	0.8578±0.0091	0.9161±0.0046	0.9664±0.0007	0.9945±0.0003
	data	0.5938±0.0868	0.7715±0.0104	0.8642±0.0055	0.9630±0.0007	0.9927±0.0003
	SF(data/mc)	0.7884±0.1462	0.8993±0.0154	0.9434±0.0077	0.9965±0.0010	0.9982±0.0004
id	mc	0.9744±0.0358	0.9819±0.0037	0.9729±0.0028	0.9616±0.0007	0.9577±0.0007
	data	0.9500±0.0487	0.9724±0.0045	0.9741±0.0027	0.9597±0.0008	0.9550±0.0008
	SF(data/mc)	0.9750±0.0615	0.9903±0.0060	1.0012±0.0040	0.9980±0.0011	0.9971±0.0011
Total	SF(iso X id)	0.7687±0.1506	0.8906±0.0162	0.9445±0.0086	0.9945±0.0015	0.9953±0.0012

Table 8: Muon isolation and identification efficiencies measured with the tag&probe method. The uncertainties are statistical only.

6 Data Driven Background Estimation Methods

We have developed two data-driven methods to estimate the two potentially dominant backgrounds. The first method provides an estimate of the number of events with fake leptons (jets misidentified as leptons). The second method is used to estimate the number of genuine leptons reconstructed with an incorrect charge sign.

6.1 Data Driven prediction for fake lepton backgrounds

We predict the background from fake leptons using the technique previously implemented in 2010 data analysis and documented in [2]. The idea is to count the number of events for which one lepton passes all final selections and a second lepton fails the nominal requirements but passes a looser set of requirements. We refer to the former lepton as a "numerator" lepton (n), and the latter a "non-numerator" (denominator and not numerator, or $\bar{n}$). The denominator objects are also referred to as fakeable objects (FO). The ratio of "numerator" to "denominator" objects is called a "fake rate", FR (also known as tight-to-loose ratio, TL). A fake rate function is measured in an independent data sample of multijet events. This fake rate function is measured in bins of lepton p_T and $|\eta|$, separately for electrons and muons.

The numerator selections are detailed in Section 3. The denominator selections are described below, specifying only looser selections.

Muon denominator definition is to relax the following muon requirements from Section 3:

- χ^2/ndof of global fit < 50 (was < 10);
- transverse impact parameter with respect to the selected vertex is < 2 mm (was < 200 μm);
- Iso is set to be $Iso < 0.4$ (was < 0.15).

Electron denominator definition is to relax the following electron requirements from Section 3:

- the impact parameter cut is removed (was < 200 μm);
- Iso is set to be $Iso < 0.6$ (was < 0.15).

This is analogous to the V3 denominator in [2] used for our previous analysis.

We thus use an extrapolation in isolation (and impact parameter) to estimate the fake lepton backgrounds in both electrons and muons. This choice is driven by the expectation that the selected events with fake leptons are dominated by heavy flavor jets, in which the lepton candidate is predominantly a real lepton from b/c-quark semileptonic decays. Relaxed isolation and impact parameter selections are then expected to roughly keep the same sample composition in events with denominator leptons.

Samples of multijet (inclusive QCD) events in data are selected among events with a single lepton trigger present. The samples and the triggers used in this measurement are listed in Section 2. Since essentially all of the dilepton analysis events are collected on dilepton-triggered events, the most appropriate choice for the FR measurement is to use triggers based on the same (or almost the same) single-object triggers as the signal selection dilepton triggers. The single-lepton triggered events are required to have an electron or a muon passing the denominator requirements described above. These events are further pruned of the contamination from the electroweak processes with W or Z production. The W events are suppressed by a requirement that $\not\!\!E_T$ is below 20 GeV and the transverse mass $M_T < 25$ GeV. The Z events are suppressed by removing dielectron and dimuon events with another lepton matching the fakeable object and forming a pair with an invariant mass within the 71 to 111 GeV range (events are removed only with dileptons with both $p_T > 20$ GeV and the other lepton passing a looser ID and isolation selection of the early $t\bar{t}$ analysis [2]).

We repeat all the studies performed with 2010 data, as documented in [2]. These include

- extraction of the fake rates in simulation and data;
- closure tests on W+jet, $t\bar{t}$, and double-fake QCD events;
- measurement of the fake-rate dependence on the *opposite-side* jet p_T, as a measure of the dependence on the progenitor parton momentum;
- estimates of the residual W+jet and Z contamination in the sample;
- comparison with the fake rate measured in events with enhanced heavy flavor contribution using b-tagging (the variation observed here is up to about 20% for electrons and muons in both simulation and data).

We arrive to essentially the same conclusions on the performance of the fake-rate method as we did in the past. In particular, we find that the method works reasonably well, still with a systematic uncertainty of about 50%. In the following we summarize the measurement of the fake rate and provide several highlights of the studies with the current dataset.

The nominal fake rates are measured requiring an "opposite side" jet with $p_T > 40$ GeV, separated by $\Delta R > 1.0$ from the FO. The electron fake rates are measured separately for triggers with an isolation requirement and for triggers without any isolation requirement on the electron. Results of the measurement are summarized in Tables 9 and 10 for the case with and without isolation requirement, respectively. The muon fake rates are measured using all single-muon triggers described in Section 2. The measurement is summarized in Table 11.

$|\eta|$ \ p_T	10 – 15	15 – 20	20 – 25	25 – 35	35 – 55
0.000 – 1.000	0.2820 ± 0.0110	0.1903 ± 0.0110	0.1862 ± 0.0114	0.1901 ± 0.0122	0.2905 ± 0.0215
1.000 – 1.479	0.2929 ± 0.0189	0.2147 ± 0.0188	0.2128 ± 0.0170	0.2003 ± 0.0167	0.3111 ± 0.0282
1.479 – 2.000	0.2651 ± 0.0242	0.1922 ± 0.0208	0.1969 ± 0.0142	0.1902 ± 0.0139	0.2478 ± 0.0200
2.000 – 2.500	0.2790 ± 0.0212	0.2687 ± 0.0233	0.2531 ± 0.0171	0.2634 ± 0.0161	0.3404 ± 0.0219

Table 9: Electron fake rate measured in bins of the electron candidate p_T and η for electrons collected using triggers with isolation requirement. The uncertainties are statistical only.

$|\eta|$ \ p_T	10 – 15	15 – 20	20 – 25	25 – 35	35 – 55
0.000 – 1.000	0.2234 ± 0.0217	0.1746 ± 0.0276	0.1228 ± 0.0307	0.1444 ± 0.0371	0.3400 ± 0.0670
1.000 – 1.479	0.2136 ± 0.0404	0.1867 ± 0.0450	0.1739 ± 0.0559	0.2353 ± 0.0594	0.3810 ± 0.1060
1.479 – 2.000	0.2241 ± 0.0548	0.2326 ± 0.0644	0.1528 ± 0.0424	0.2308 ± 0.0477	0.3409 ± 0.0715
2.000 – 2.500	0.2432 ± 0.0499	0.4038 ± 0.0680	0.1455 ± 0.0475	0.3182 ± 0.0573	0.3529 ± 0.0820

Table 10: Electron fake rate measured in bins of the electron candidate p_T and η for electrons collected using triggers without isolation requirements. The uncertainties are statistical only.

$|\eta|$ \ p_T	5 – 10	10 – 15	15 – 20	20 – 25	25 – 35
0.000 – 1.000	0.2810 ± 0.0028	0.2205 ± 0.0025	0.1968 ± 0.0033	0.1725 ± 0.0045	0.1735 ± 0.0015
1.000 – 1.479	0.3106 ± 0.0039	0.2536 ± 0.0037	0.2143 ± 0.0047	0.1780 ± 0.0061	0.2033 ± 0.0023
1.479 – 2.000	0.3370 ± 0.0041	0.2730 ± 0.0039	0.2287 ± 0.0050	0.2065 ± 0.0068	0.2217 ± 0.0025
2.000 – 2.500	0.3304 ± 0.0052	0.2703 ± 0.0051	0.2039 ± 0.0062	0.1932 ± 0.0088	0.2351 ± 0.0038

Table 11: Muon fake rate measured in bins of the muon candidate p_T and η. The uncertainties are statistical only.

Figures 5 and 6 show the projection on p_T and $|\eta|$ of these fake rates for electrons and muons, respectively. Electron fake rates measured for triggers with an isolation requirement are slightly higher than those for triggers without an isolation requirement, as expected. The difference, even though it's not very large, is significant enough and we treat fake rates for these triggers separately. The dependence of the fake rates on the away-jet momentum is also shown on these figures.

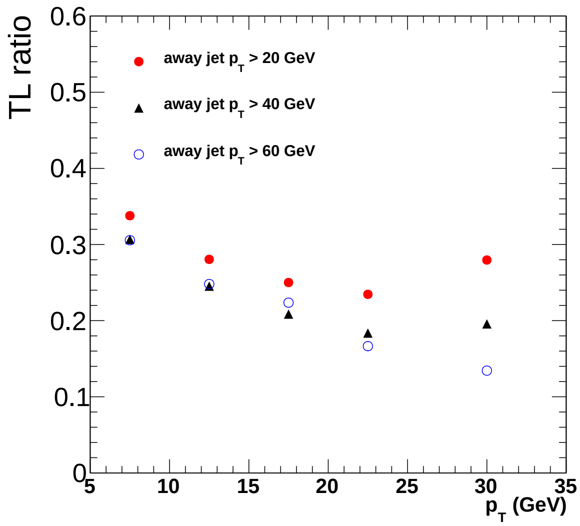

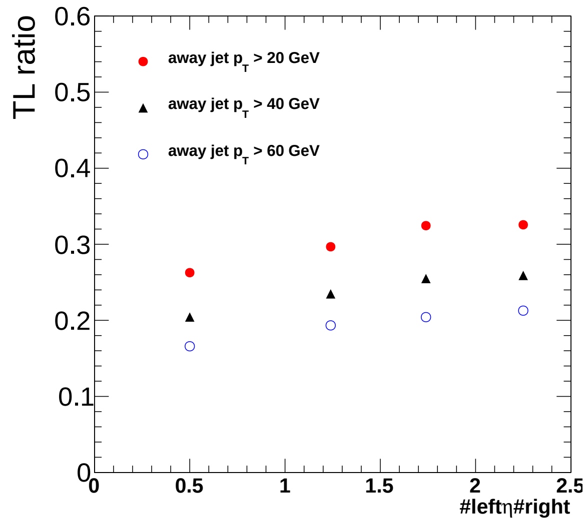

Figure 5: Muon fake rate projected on p_T (left) and $|\eta|$ (right). The fake rates are shown separately for measurements with a requirement for an away jet p_T to be above 20 GeV/c (red circles), 40 GeV/c (black circles), and 60 GeV/c (blue circles).

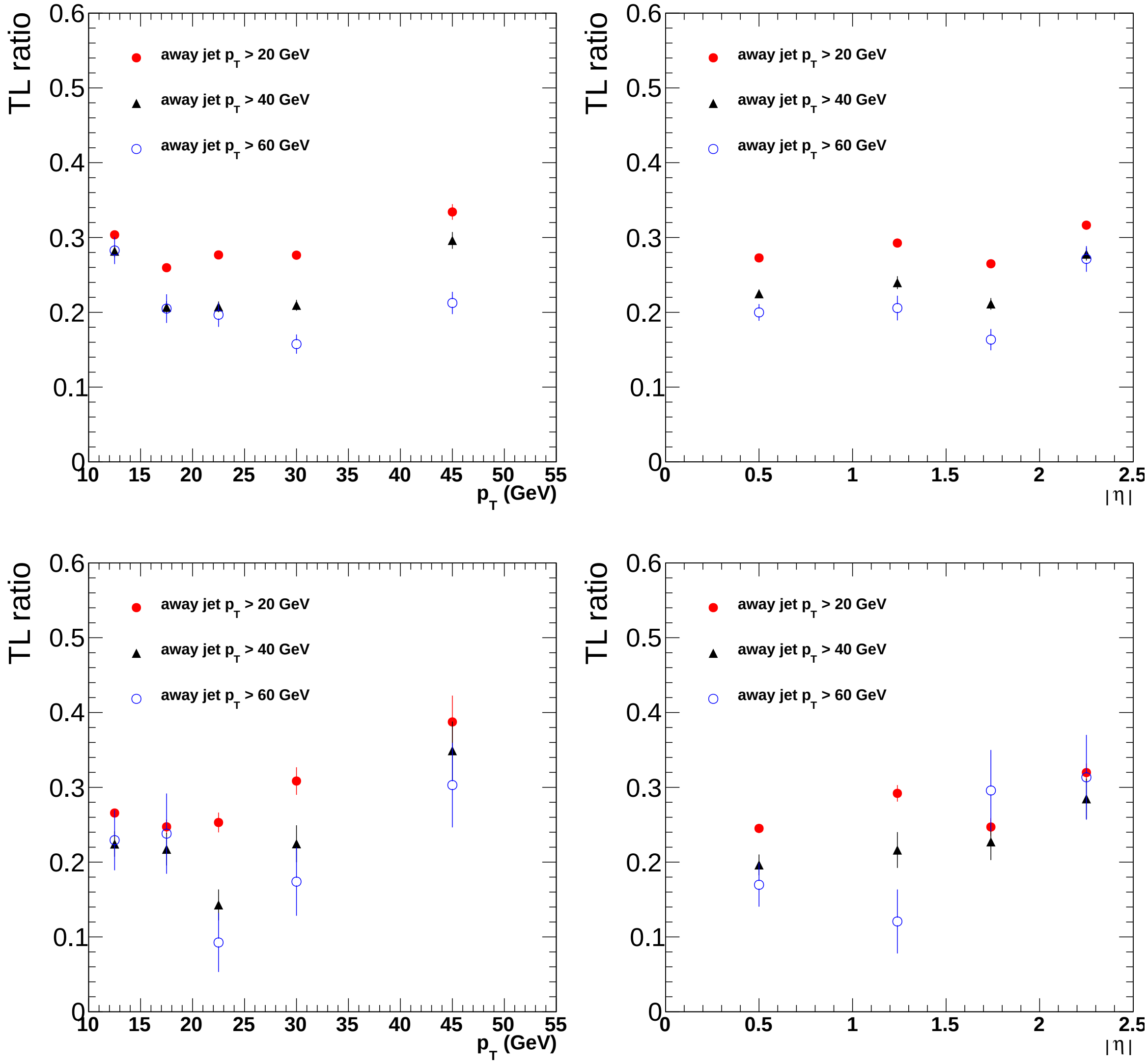

Figure 6: Electron fake rate projected on p_T (left) and $|\eta|$ (right) for electrons collected by the triggers with isolation requirement (top) and without it (bottom). The fake rates are shown separately for measurements with a requirement for an away jet p_T to be above 20 GeV$/c$ (red filled circles), 40 GeV$/c$ (black up triangles), and 60 GeV$/c$ (blue open circles).

Similar to the choice made in 2010 data analysis, we restrict the measurement of the fake rate to 35 GeV/c(55 GeV/c) for muons (electrons) in order to avoid the residual contribution from the W+jets and Z events. We find that the contribution from the W/Z production is small for electrons up to about 55 GeV, as illustrated in Fig. 7 for data (left) and simulation (right), respectively. There is no significant contribution from the W events in the MC, which is supported by only marginal increase in the fake rate in data after the W suppression requirements are removed. For muons, since the selection did not change significantly, we refer to the corresponding figure in [2].

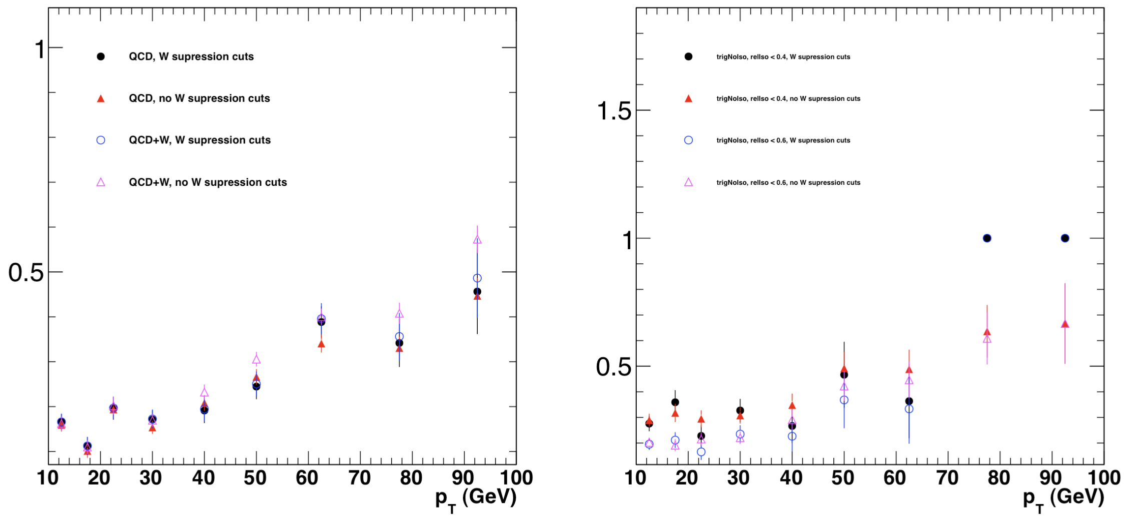

Figure 7: Electron fake rate as a function of the electron p_T measured for a range of selection enhancing the contribution from the W/Z events. The fake rate measured in data (left) is shown for the nominal measurement (open circles), the measurement without additional W suppression (open up triangles), as well as for a selection with a tighter isolation requirement of $Iso < 0.4$ with (black filled circles) and without the W suppression (up red triangles). Fake rates for bins with no entries are (incidentally) reported with a value of 1.0. The electron fake rate measured in MC (left) is shown for the nominal measurement using only QCD samples (filled circles), and that with the W sample included (open circles), as well as for the selection without the W suppression measured in the QCD sample alone (filled triangles) and that with the W sample included (open triangles).

The following assumptions are made prior to applying the measured fake rates to the dilepton events.

- The fake rate per lepton is independent for the two leptons, e.g. to predict the fake contribution to an $e\mu$ final state we consider electron and muon fakes separately, and add them up, assuming no correlations between the two estimates.
- We assume the lepton fake rate measurement in an inclusive QCD sample as described in [2] represents the lepton fake rate in the dilepton sample.

We test that the fake rates measured in QCD are applicable to the dilepton samples by performing closure tests on simulated W+jets, $t\bar{t}$, and QCD samples. The tests done on W+jets and $t\bar{t}$ samples are done as follows

1. select events passing the baseline selections;
2. require that one lepton is matched to a leptonic W decay and the other (fake) lepton is not matched to a leptonic W decay;
3. scale the number of fake leptons failing the full lepton selections and passing the FO selections by $FR/(1-FR)$ as a function of the fake lepton p_T and $|\eta|$ — this is the prediction of the number of fakes passing full lepton selections;
4. compare the predicted and observed number of fake leptons.

The prediction of the number of events with fakes gives a consistent overestimate for the $t\bar{t}$ events for both electrons and muons by approximately 70%. We attribute this to the difference in the underlying parton momenta in $t\bar{t}$ and inclusive QCD events: the momentum is generally higher in $t\bar{t}$ events, which corresponds to a smaller effective fake rate. We find that the prediction of the number of fakes gives a marginally significant underestimate for W+jets events. The statistical uncertainty of this test is much larger for muons than for electrons. We expect this to happen if the jets initiating the fakes in W+jet events have a smaller momentum on average compared to those used to extract the fake rate in QCD events. Results of the closure tests on $t\bar{t}$ and W+jet events passing the baseline selections of *high-p_T* dileptons are summarized in Table 12. In addition to this, we have performed a closure test on the same-sign dimuon events in the QCD sample (without any additional requirement on the number of jets or on $\not\!\!E_T$): we find that the number of expected events agrees with the observed within statistical uncertainty of about 20%.

Sample	result	ElectronFR		Muon FR	
		ee	$e\mu$	$\mu\mu$	$e\mu$
$t\bar{t}$	observed	2.8 ± 0.2	4.2 ± 0.2	3.9 ± 0.2	4.0 ± 0.2
	predicted	4.9 ± 0.4	6.8 ± 0.5	7.2 ± 0.3	6.5 ± 0.2
	ratio	1.8 ± 0.2	1.6 ± 0.2	1.8 ± 0.1	1.6 ± 0.1
W+jets	observed	< 2.1	8.4 ± 4.2	2.1 ± 2.1	
	predicted	1.5 ± 0.8	3.4 ± 1.4	2.1 ± 1.2	
	ratio	< 1.4	0.4 ± 0.3	1.0 ± 1.2	

Table 12: Fake rate closure test on $t\bar{t}$ and W+jets events for high-p_T dilepton selections. The muon FR test in $e\mu$ is done with $\not\!\!E_T > 20$ GeV. The number of events is scaled to 1 fb^{-1}. Expcept for the test in $t\bar{t}$ with electrons (done with jet $p_T > 40$ GeV), the results are reported for events with at least two jets with $p_T > 30$ GeV (old selection), used to increase the number of events passing the selections.

An estimate of the number of fake leptons in dilepton events passing full (numerator) selections is based on counts of dilepton events with two non-numerator $N_{\overline{nn}}$, two numerator N_{nn}, and only one non-numerator object $N_{n\overline{n}}$. Assuming $N_{\overline{nn}}$ is dominated by QCD (both leptons are fake), a relatively simple calculation leads to the following, neglecting much smaller terms. The QCD contribution to the signal sample N_{nn}^{QCD} is given by

$$N_{nn}^{QCD} = \sum_{i,j} \frac{FR_i FR_j}{(1 - FR_i)(1 - FR_j)} N_{\overline{nn}}^{ij},$$

where the indices i, j correspond to the binning and flavor of corresponding non-numerator lepton objects. The contribution from one true and one fake lepton (e.g. $t\bar{t}$, single top, Wjets) contribution in the signal sample N_{nn}^{W} is given by

$$N_{nn}^{W,raw} = \sum_{i} \frac{FR_i}{(1 - FR_i)} N_{n\overline{n}}^{i},$$

$$N_{nn}^{W} = N_{nn}^{W,raw} - 2N_{nn}^{QCD}.$$

The total prediction of the number of events with fake leptons is thus

$$N_{nn}^{fakes} = N_{nn}^{W} + N_{nn}^{QCD}.$$

The systematic uncertainty of $\pm 50\%$ per fake lepton is estimated for the fake rate method. It is justified based on the closure tests and an understanding that the variation of the fake rate on the jet momentum corresponds to the variation between the fakes from the ISR/FSR jets (like in W+jets), and jets from the heavy final states (as in $t\bar{t}$). We compute the contributions from QCD and W+jets and assign a 50% systematic uncertainty on the combined estimate.

We have neglected any ”signal contamination”. Signal contamination enters when there is a significant source of two isolated leptons, with one or both failing the numerator cuts, but passing the denominator cuts comprising a significant fraction of the total number of $N_{n\overline{n}}$ or $N_{\overline{nn}}$ samples. As we see no evidence of any signal excess, we can safely ignore this.

6.2 Data Driven prediction for charge mis-reconstruction backgrounds

Following our original studies [9] of the electron charge misreconstruction, we apply the requirement for electrons that all three charge measurements for a GSF electron agree. This dramatically reduces the rate of charge mis-measurement for electrons to the point where it is an almost negligible source of background, less than 10% of the background due to fake leptons, as was shown in the 2010 analysis [20]. Even though this background is small, it is not necessarily well-reproduced in simulation. We apply a data-driven method used in the previous analysis here.

The following steps are done:

1. Measure the probability for an electron to have its charge misreconstructed in bins of $|\eta|$ and p_T using single electron gun Monte Carlo.

2. Use this probability and apply it to the opposite sign Z sample for a Z control sample defined as 76 GeV $< m_{ll} <$ 106 GeV, $\not\!\!E_T <$ 20 GeV, and transverse mass $<$ 25 GeV. Here transverse mass is calculated based on whichever lepton has higher p_T. Compare with the actual yield of double-charged Z candidates in that region to establish validity of the approach.

3. If the expected and observed yields agree reasonably well in the previous step, continue using the probability measured in the first step and use the discrepancy as the systematic uncertainty.

4. Then apply this probability to all the electrons in opposite sign dilepton events that pass the selection. This produces the data driven charge flip prediction shown in the tables in Section 8.

Figure 8 shows the p_T (left) and $|\eta|$ (right) projections of the charge mismeasurement probability from single electron gun Monte Carlo. The same function is applied to data and MC. As seen in Fig. 8 (right), the charge mismeasurement probability did not change substantially in the samples used for the previous analysis, as well as for the Spring11 and Summer11 simulation.

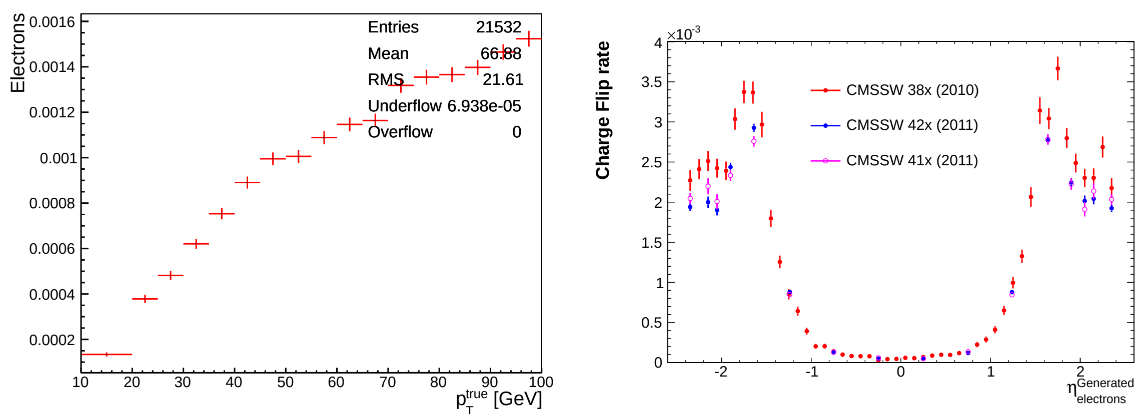

Figure 8: Charge mismeasurement probability from single electron gun MC shown in projections on p_T (left) and η (right). The projection on η also shows the distributions for the charge mismeasurement probability in 2010 analysis (red), current definition (blue), and that in the older (Spring11-like) MC sample.

We find 129 events with same-sign electron pairs in data in the Z control region, compared to an expectation of 100.0 ± 0.3 events from the opposite-sign dielectron sample and 8 ± 4 events from fake electrons. The number of events expected directly from simulation is 94 ± 10. The same-sign dielectron mass distribution observed in data is compared to the expectation from simulation in Fig. 9. These comparisons are consistent within statistics. Based on these observations we assign a correction factor of 1.2 ± 0.2 to the expected number of same-sign dielectron events obtained using the opposite-sign dielectron samples. The scale factor corresponds to the relative difference between $121 \pm 11(\mathrm{stat.}) \pm 4(\mathrm{syst})$ and 100 ± 0.3, the uncertainty is taken to be 20% to account in addition for potential effects not covered by this test with Z events.

7 Definition of the signal region

We define a signal region to look for possible new physics contributions in the same sign isolated dilepton sample. The choice of signal region is driven by three observations:

1. astrophysical evidence for dark matter suggests that we concentrate on the region of high $\not\!\!E_T$;

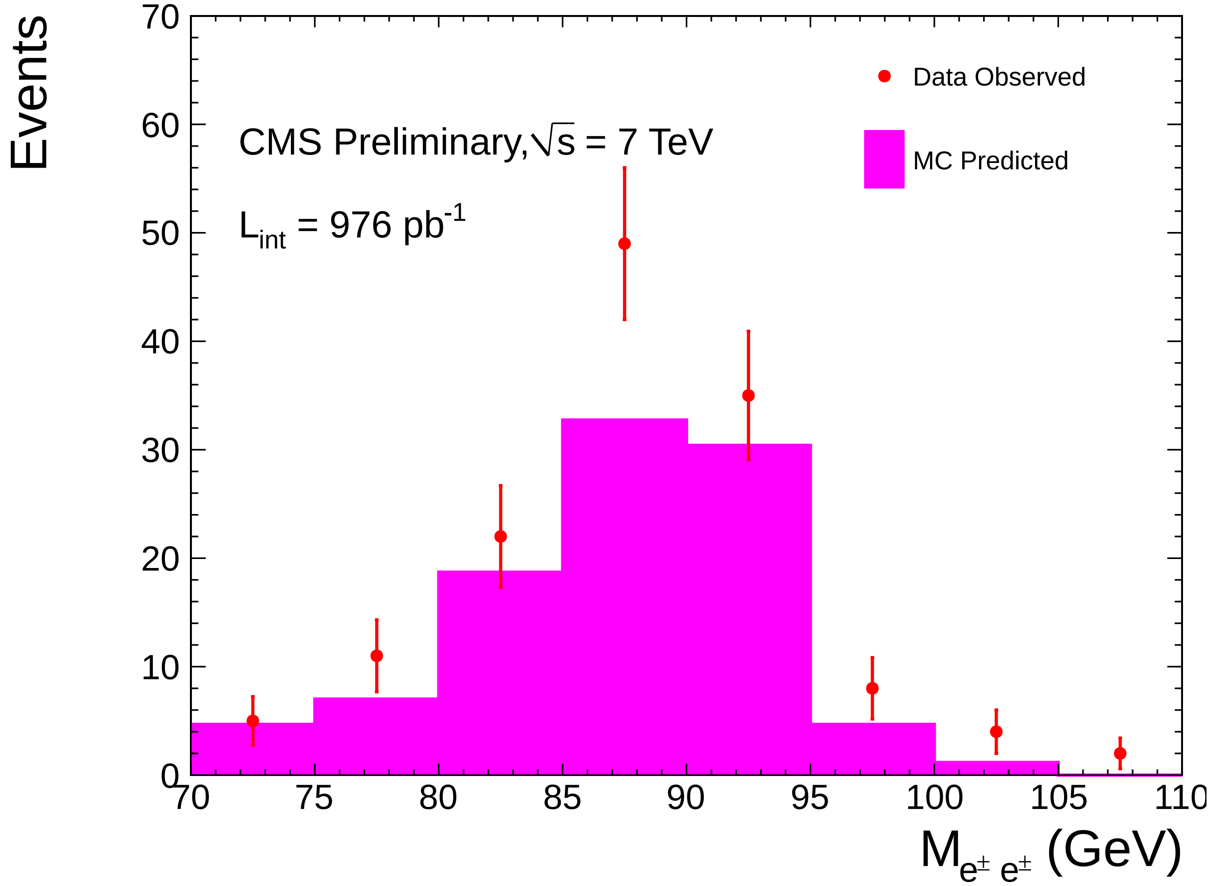

Figure 9: Same sign ee invariant mass distribution compared with $Z \to ee$ Monte Carlo expectations. Cuts on missing transverse energy $<$ 20 GeV and transverse mass $<$ 25 GeV have been applied to reduce backgrounds from $W+$ jets. The highest p_T lepton has been used in the calculation of the transverse mass.

2. new physics signals should have high $\sqrt{\hat{s}}$;

3. observable high cross section new physics signals are likely to be produced strongly; thus, we expect significant hadronic activity in conjunction with the two leptons.

Following these observations, we define signal regions in the H_T vs $\not\!\!E_T$ plane in addition to the baseline requirements of Section 3. Several (inclusive) regions are identified in the H_T-$\not\!\!E_T$ plane following estimates of an optimal sensitivity to new physics models, as described in [4]:

- $H_T > 400$ GeV and $\not\!\!E_T > 120$ GeV, inspired by mSUGRA model with low m_0;
- $H_T > 400$ GeV and $\not\!\!E_T > 50$ GeV, inspired by mSUGRA model with high m_0 (here the cascade decays from the initial squarks and gluinos are boosted significantly in opposite directions and the momenta of the LSPs partially cancel);
- $H_T > 200$ GeV and $\not\!\!E_T > 120$ GeV, useful for tests of sensitivity to a simplified model of squark-gluino production [23];
- $H_T > 80$ GeV and $\not\!\!E_T > 100$ GeV, inspired by the pMSSM model with sneutrino LSP (meaningful only for the *high-*p_T dilepton selections).

In order to cover the phase space of the possible new physics final states, we report results separately for the *high-*p_T and *low-*p_T dilepton selections. Note that the H_T requirement (200 GeV) is motivated by the trigger turn-on curves for the dilepton plus H_T triggers described in Section 4. We choose the same H_T requirement for the "high

P_T" leptons triggered via leptonic triggers for consistency. We further argue that the most efficient combination given a specific signal model can be performed with the data yields (and expectations) separated into mutually exclusive regions in the dilepton momentum space as well as in the H_T-$\not\!\!E_T$ space. The simplest partitioning in the H_T-$\not\!\!E_T$ space can be done along the $H_T = 200$ GeV, and 400 GeV, and along $\not\!\!E_T = 50$ GeV and 120 GeV. This separation can be done based on the yields reported for the inclusive selections described above.

8 Results

In the following we report yields of events observed in data and compare them to the predictions from the data-driven methods as well as from simulation. These results are reported for *high-*p_T and *low-*p_T dilepton selections with H_T and $\not\!\!E_T$ selected as defined in the baseline selection described in Section 3, as well as for the signal regions defined in Section 7. As anticipated, the MC predicts that $t\bar{t}$ is the largest background in all cases. The data yield is in good agreement with the prediction from both MC as well as the data driven prediction. The procedure for arriving at these data driven predictions is detailed in Section 6. These data-driven predictions supersede all the MC estimates of the contributions from events with fake leptons or with leptons with misreconstructed charge. The remaining MC contribution in the final estimates of background events are those with real leptons: $WZ \to lll\nu$, $ZZ \to llll$; same-sign W from single-parton (spWW), double-parton (dpWW), and $t\bar{t}W$ production. Note that we have also included a contribution from W/Z+γ background events where the asymmetric conversion of the photon can give rise to an electron of the same sign as a lepton from W or Z. This background is not predicted by the fake lepton prediction method. Results of background estimates in simulation and data are compared with the number of observed events in data in the tables below. The SUSY LM6 point yield based on the LO cross section is provided as a reference. The NLO/LO k-factor for LM6 is 1.3 [5].

Source	ee	$\mu\mu$	eμ	all
$t\bar{t} \rightarrow \ell\ell X$	0.996 ± 0.448	0.000 ± 0.144	0.746 ± 0.417	1.742 ± 0.612
$t\bar{t} \rightarrow \ell(b \rightarrow \ell)X$	3.545 ± 0.850	3.514 ± 0.830	5.634 ± 1.067	12.692 ± 1.597
$t\bar{t} \rightarrow \ell(\not{b} \rightarrow \ell)X$	1.832 ± 0.571	0.000 ± 0.144	0.821 ± 0.407	2.653 ± 0.701
$t\bar{t}$ other	0.000 ± 0.144	0.000 ± 0.144	0.000 ± 0.144	0.000 ± 0.144
tW	0.234 ± 0.084	0.121 ± 0.053	0.348 ± 0.098	0.703 ± 0.139
t, t-channel	0.173 ± 0.088	0.117 ± 0.076	0.458 ± 0.171	0.749 ± 0.206
t, s-channel	0.023 ± 0.010	0.007 ± 0.005	0.020 ± 0.009	0.049 ± 0.014
W+jets	0.000 ± 2.039	0.000 ± 2.039	4.117 ± 2.636	4.117 ± 2.636
$Z \rightarrow ee$	0.000 ± 1.169	0.000 ± 1.169	0.000 ± 1.169	0.000 ± 1.169
$Z \rightarrow \mu\mu$	0.000 ± 1.169	0.000 ± 1.169	0.000 ± 1.169	0.000 ± 1.169
$Z \rightarrow \tau\tau$	0.000 ± 1.169	0.000 ± 1.169	0.000 ± 1.169	0.000 ± 1.169
WW	0.000 ± 0.040	0.000 ± 0.040	0.000 ± 0.040	0.000 ± 0.040
WZ	0.536 ± 0.076	0.689 ± 0.091	1.132 ± 0.112	2.357 ± 0.164
ZZ	0.055 ± 0.015	0.051 ± 0.014	0.112 ± 0.020	0.218 ± 0.029
Vγ	1.066 ± 0.542	0.000 ± 0.210	0.428 ± 0.335	1.494 ± 0.637
spW^+W^+	0.409 ± 0.022	0.598 ± 0.027	0.997 ± 0.035	2.005 ± 0.049
spW^-W^-	0.131 ± 0.006	0.202 ± 0.008	0.330 ± 0.010	0.662 ± 0.014
dp$W^\pm W^\pm$	0.004 ± 0.003	0.011 ± 0.005	0.013 ± 0.005	0.028 ± 0.007
$t\bar{t}W$	0.839 ± 0.018	1.301 ± 0.022	2.178 ± 0.029	4.317 ± 0.041
Total MC	9.841 ± 1.251	6.611 ± 0.841	17.333 ± 2.932	33.786 ± 3.296
LM6	1.018 ± 0.043	1.334 ± 0.050	2.223 ± 0.064	4.576 ± 0.092
Prompt-fake	13.67 ± 2.32	14.18 ± 2.21	30.08 ± 3.99	57.93 ± 5.12
Double-fake	0.62 ± 0.21	1.11 ± 0.27	2.24 ± 0.50	3.97 ± 0.60
Total with fakes	14.29 ± 2.29 ± 7.15	15.29 ± 2.16 ± 7.65	32.32 ± 3.90 ± 16.16	61.90 ± 5.01 ± 30.95
Charge misreconstruction	1.77 ± 0.08 ± 0.35	- ± -	0.71 ± 0.04 ± 0.14	2.48 ± 0.09 ± 0.50
Simulated backgrounds	3.04 ± 0.55 ± 1.52	2.85 ± 0.10 ± 1.43	5.19 ± 0.36 ± 2.59	11.08 ± 0.66 ± 5.54
All backgrounds	11.04 ± 2.22 ± 4.52	20.90 ± 3.41 ± 9.61	25.63 ± 3.30 ± 11.32	57.57 ± 5.24 ± 25.45
Data	16	16	24	56

Table 13: Observed event yields in baseline ($\not{E}_T >$ 30 GeV, and at least 2 jets with pT $>$ 40 GeV) high-p_T (pT $>$ 20/10) dileptons compared to expectations from simulation alone, and from the data-driven methods. The *simulated backgrounds* contribution includes contributions from genuine same-sign lepton pairs (WZ, ZZ, leptons from same-sign W from single-parton, double-parton, and $t\bar{t}W$ production), as well as electrons from converted photons in $V\gamma$ production. Entries with zero contributing events are reported with an uncertainty corresponding to one event. This uncertainty is not added to the total MC contribution. Systematic uncertainties (the second uncertainty if present) are displayed only for the final combined type of background, no systematic uncertainty is added for estimates with zero entries. Systematic uncertainties are 100% correlated among the channels.

Source	ee	$\mu\mu$	eμ	all
$t\bar{t} \to \ell\ell X$	0.000 $\pm$ 0.144	0.000 $\pm$ 0.144	0.000 $\pm$ 0.144	0.000 $\pm$ 0.144
$t\bar{t} \to \ell(b \to \ell)X$	0.000 $\pm$ 0.144	0.000 $\pm$ 0.144	0.216 $\pm$ 0.216	0.216 $\pm$ 0.216
$t\bar{t} \to \ell(\not{b} \to \ell)X$	0.000 $\pm$ 0.144	0.000 $\pm$ 0.144	0.000 $\pm$ 0.144	0.000 $\pm$ 0.144
$t\bar{t}$ other	0.000 $\pm$ 0.144	0.000 $\pm$ 0.144	0.000 $\pm$ 0.144	0.000 $\pm$ 0.144
tW	0.000 $\pm$ 0.021	0.000 $\pm$ 0.021	0.000 $\pm$ 0.021	0.000 $\pm$ 0.021
t, t-channel	0.015 $\pm$ 0.042	0.000 $\pm$ 0.042	0.000 $\pm$ 0.042	0.015 $\pm$ 0.042
t, s-channel	0.000 $\pm$ 0.003	0.000 $\pm$ 0.003	0.000 $\pm$ 0.003	0.000 $\pm$ 0.003
W+jets	0.000 $\pm$ 2.039	0.000 $\pm$ 2.039	0.000 $\pm$ 2.039	0.000 $\pm$ 2.039
$Z \to ee$	0.000 $\pm$ 1.169	0.000 $\pm$ 1.169	0.000 $\pm$ 1.169	0.000 $\pm$ 1.169
$Z \to \mu\mu$	0.000 $\pm$ 1.169	0.000 $\pm$ 1.169	0.000 $\pm$ 1.169	0.000 $\pm$ 1.169
$Z \to \tau\tau$	0.000 $\pm$ 1.169	0.000 $\pm$ 1.169	0.000 $\pm$ 1.169	0.000 $\pm$ 1.169
WW	0.000 $\pm$ 0.040	0.000 $\pm$ 0.040	0.000 $\pm$ 0.040	0.000 $\pm$ 0.040
WZ	0.006 $\pm$ 0.006	0.000 $\pm$ 0.008	0.056 $\pm$ 0.026	0.062 $\pm$ 0.027
ZZ	0.000 $\pm$ 0.003	0.000 $\pm$ 0.003	0.000 $\pm$ 0.003	0.000 $\pm$ 0.003
Vγ	0.000 $\pm$ 0.210	0.000 $\pm$ 0.210	0.000 $\pm$ 0.210	0.000 $\pm$ 0.210
spW^+W^+	0.047 $\pm$ 0.008	0.069 $\pm$ 0.009	0.141 $\pm$ 0.013	0.256 $\pm$ 0.018
spW^-W^-	0.011 $\pm$ 0.002	0.016 $\pm$ 0.002	0.024 $\pm$ 0.003	0.052 $\pm$ 0.004
dp$W^\pm W^\pm$	0.000 $\pm$ 0.002	0.000 $\pm$ 0.002	0.000 $\pm$ 0.002	0.000 $\pm$ 0.002
$t\bar{t}W$	0.045 $\pm$ 0.004	0.082 $\pm$ 0.006	0.137 $\pm$ 0.007	0.264 $\pm$ 0.010
Total MC	0.126 $\pm$ 0.019	0.167 $\pm$ 0.011	0.574 $\pm$ 0.219	0.867 $\pm$ 0.220
LM6	0.804 $\pm$ 0.039	1.043 $\pm$ 0.044	1.712 $\pm$ 0.056	3.559 $\pm$ 0.081
Prompt-fake	0.25 $\pm$ 0.59	0.22 $\pm$ 0.56	0.31 $\pm$ 0.76	0.77 $\pm$ 0.83
Double-fake	0.00 $\pm$ 0.27	0.00 $\pm$ 0.26	0.00 $\pm$ 0.34	0.00 $\pm$ 0.34
Total with fakes	0.25 $\pm$ 0.25 $\pm$ 0.13	0.22 $\pm$ 0.22 $\pm$ 0.11	0.31 $\pm$ 0.32 $\pm$ 0.15	0.77 $\pm$ 0.46 $\pm$ 0.39
Charge misreconstruction	0.012 $\pm$ 0.006 $\pm$ 0.002	- $\pm$ -	0.014 $\pm$ 0.006 $\pm$ 0.003	0.026 $\pm$ 0.008 $\pm$ 0.005
Simulated backgrounds	0.110 $\pm$ 0.011 $\pm$ 0.055	0.167 $\pm$ 0.011 $\pm$ 0.083	0.358 $\pm$ 0.030 $\pm$ 0.179	0.635 $\pm$ 0.034 $\pm$ 0.317
All backgrounds	0.37 $\pm$ 0.25 $\pm$ 0.14	0.38 $\pm$ 0.22 $\pm$ 0.14	0.68 $\pm$ 0.33 $\pm$ 0.24	1.44 $\pm$ 0.47 $\pm$ 0.50
Data	0	0	0	0

Table 14: Observed event yields in high-p_T (pT > 20/10) dileptons passing the *low-m_0* signal selections ($H_T >$ 400 GeV, $\not{E}_T$> 120 GeV) compared to expectations from simulation alone, and from the data-driven methods. The *simulated backgrounds* contribution includes contributions from genuine same-sign lepton pairs (WZ, ZZ, leptons from same-sign W from single-, double-parton, and $t\bar{t}W$ production), as well as electrons from converted photons in $V\gamma$ production. Entries with zero contributing events are reported with an uncertainty corresponding to one event. This uncertainty is not added to the total MC contribution. Systematic uncertainties (the second uncertainty if present) are displayed only for the final combined type of background, no systematic uncertainty is added for estimates with zero entries. Systematic uncertainties are 100% correlated among the channels.

Source	ee	$\mu\mu$	eμ	all
$t\bar{t} \to \ell\ell X$	0.000 ± 0.144	0.000 ± 0.144	0.000 ± 0.144	0.000 ± 0.144
$t\bar{t} \to \ell(b \to \ell)X$	0.255 ± 0.255	0.111 ± 0.111	0.216 ± 0.216	0.583 ± 0.353
$t\bar{t} \to \ell(\not{b} \to \ell)X$	0.255 ± 0.255	0.000 ± 0.144	0.247 ± 0.219	0.502 ± 0.336
$t\bar{t}$ other	0.000 ± 0.144	0.000 ± 0.144	0.000 ± 0.144	0.000 ± 0.144
tW	0.000 ± 0.021	0.000 ± 0.021	0.000 ± 0.021	0.000 ± 0.021
t, t-channel	0.015 ± 0.042	0.000 ± 0.042	0.000 ± 0.042	0.015 ± 0.042
t, s-channel	0.000 ± 0.003	0.000 ± 0.003	0.000 ± 0.003	0.000 ± 0.003
W+jets	0.000 ± 2.039	0.000 ± 2.039	0.000 ± 2.039	0.000 ± 2.039
$Z \to ee$	0.000 ± 1.169	0.000 ± 1.169	0.000 ± 1.169	0.000 ± 1.169
$Z \to \mu\mu$	0.000 ± 1.169	0.000 ± 1.169	0.000 ± 1.169	0.000 ± 1.169
$Z \to \tau\tau$	0.000 ± 1.169	0.000 ± 1.169	0.000 ± 1.169	0.000 ± 1.169
WW	0.000 ± 0.040	0.000 ± 0.040	0.000 ± 0.040	0.000 ± 0.040
WZ	0.013 ± 0.009	0.021 ± 0.016	0.062 ± 0.027	0.096 ± 0.032
ZZ	0.000 ± 0.003	0.001 ± 0.001	0.000 ± 0.003	0.001 ± 0.001
Vγ	0.000 ± 0.210	0.000 ± 0.210	0.000 ± 0.210	0.000 ± 0.210
spW^+W^+	0.102 ± 0.011	0.132 ± 0.013	0.271 ± 0.018	0.506 ± 0.025
spW^-W^-	0.026 ± 0.003	0.034 ± 0.003	0.059 ± 0.004	0.119 ± 0.006
dp$W^\pm W^\pm$	0.000 ± 0.002	0.000 ± 0.002	0.002 ± 0.002	0.002 ± 0.002
$t\bar{t}W$	0.113 ± 0.007	0.172 ± 0.008	0.300 ± 0.011	0.586 ± 0.015
Total MC	0.780 ± 0.362	0.473 ± 0.113	1.157 ± 0.310	2.410 ± 0.489
LM6	0.864 ± 0.040	1.122 ± 0.046	1.872 ± 0.058	3.858 ± 0.084
Prompt-fake	1.06 ± 0.76	0.97 ± 0.77	0.59 ± 0.81	2.62 ± 1.13
Double-fake	0.00 ± 0.27	0.00 ± 0.26	0.00 ± 0.34	0.00 ± 0.34
Total with fakes	1.06 ± 0.54 ± 0.53	0.97 ± 0.57 ± 0.48	0.59 ± 0.43 ± 0.30	2.62 ± 0.90 ± 1.31
Charge misreconstruction	0.064 ± 0.016 ± 0.013	- ± -	0.025 ± 0.007 ± 0.005	0.089 ± 0.017 ± 0.018
Simulated backgrounds	0.254 ± 0.016 ± 0.127	0.362 ± 0.022 ± 0.181	0.694 ± 0.034 ± 0.347	1.310 ± 0.044 ± 0.655
All backgrounds	1.38 ± 0.54 ± 0.54	1.33 ± 0.57 ± 0.52	1.31 ± 0.43 ± 0.46	4.02 ± 0.90 ± 1.46
Data	1	2	2	5

Table 15: Observed event yields in high-p_T (pT > 20/10) dileptons passing the *high-m_0* signal selections ($H_T >$ 400 GeV, $\not{E}_T >$ 50 GeV) compared to expectations from simulation alone, and from the data-driven methods. The *simulated backgrounds* contribution includes contributions from genuine same-sign lepton pairs (WZ, ZZ, leptons from same-sign W from single-, double-parton, and $t\bar{t}W$ production), as well as electrons from converted photons in $V\gamma$ production. Entries with zero contributing events are reported with an uncertainty corresponding to one event. This uncertainty is not added to the total MC contribution. Systematic uncertainties (the second uncertainty if present) are displayed only for the final combined type of background, no systematic uncertainty is added for estimates with zero entries. Systematic uncertainties are 100% correlated among the channels.

Source	ee	$\mu\mu$	eμ	all
$t\bar{t} \to \ell\ell X$	0.000 ± 0.144	0.000 ± 0.144	0.000 ± 0.144	0.000 ± 0.144
$t\bar{t} \to \ell(b \to \ell)X$	0.000 ± 0.144	0.255 ± 0.255	0.563 ± 0.326	0.819 ± 0.414
$t\bar{t} \to \ell(\not{b} \to \ell)X$	0.000 ± 0.144	0.000 ± 0.144	0.000 ± 0.144	0.000 ± 0.144
$t\bar{t}$ other	0.000 ± 0.144	0.000 ± 0.144	0.000 ± 0.144	0.000 ± 0.144
tW	0.000 ± 0.021	0.028 ± 0.020	0.000 ± 0.021	0.028 ± 0.020
t, t-channel	0.031 ± 0.022	0.000 ± 0.042	0.009 ± 0.042	0.040 ± 0.024
t, s-channel	0.000 ± 0.003	0.000 ± 0.003	0.000 ± 0.003	0.000 ± 0.003
W+jets	0.000 ± 2.039	0.000 ± 2.039	0.745 ± 2.039	0.745 ± 2.039
$Z \to ee$	0.000 ± 1.169	0.000 ± 1.169	0.000 ± 1.169	0.000 ± 1.169
$Z \to \mu\mu$	0.000 ± 1.169	0.000 ± 1.169	0.000 ± 1.169	0.000 ± 1.169
$Z \to \tau\tau$	0.000 ± 1.169	0.000 ± 1.169	0.000 ± 1.169	0.000 ± 1.169
WW	0.000 ± 0.040	0.000 ± 0.040	0.000 ± 0.040	0.000 ± 0.040
WZ	0.035 ± 0.017	0.033 ± 0.020	0.129 ± 0.039	0.197 ± 0.047
ZZ	0.005 ± 0.005	0.000 ± 0.003	0.000 ± 0.003	0.005 ± 0.005
Vγ	0.000 ± 0.210	0.000 ± 0.210	0.000 ± 0.210	0.000 ± 0.210
spW^+W^+	0.090 ± 0.010	0.132 ± 0.013	0.231 ± 0.017	0.454 ± 0.023
spW^-W^-	0.024 ± 0.003	0.037 ± 0.003	0.055 ± 0.004	0.116 ± 0.006
dp$W^\pm W^\pm$	0.000 ± 0.002	0.000 ± 0.002	0.000 ± 0.002	0.000 ± 0.002
$t\bar{t}W$	0.148 ± 0.008	0.238 ± 0.010	0.404 ± 0.012	0.790 ± 0.017
Total MC	0.333 ± 0.031	0.723 ± 0.257	2.136 ± 0.815	3.193 ± 0.855
LM6	0.899 ± 0.041	1.160 ± 0.047	1.914 ± 0.059	3.974 ± 0.086
Prompt-fake	0.90 ± 0.76	1.08 ± 0.76	0.80 ± 0.54	2.78 ± 0.95
Double-fake	0.00 ± 0.27	0.00 ± 0.26	0.09 ± 0.09	0.09 ± 0.09
Total with fakes	0.90 ± 0.54 ± 0.45	1.08 ± 0.56 ± 0.54	0.88 ± 0.52 ± 0.44	2.86 ± 0.93 ± 1.43
Charge misreconstruction	0.032 ± 0.009 ± 0.006	- ± -	0.046 ± 0.010 ± 0.009	0.078 ± 0.014 ± 0.016
Simulated backgrounds	0.302 ± 0.022 ± 0.151	0.440 ± 0.026 ± 0.220	0.819 ± 0.044 ± 0.409	1.562 ± 0.056 ± 0.781
All backgrounds	1.23 ± 0.54 ± 0.47	1.52 ± 0.56 ± 0.58	1.75 ± 0.52 ± 0.60	4.50 ± 0.93 ± 1.63
Data	0	2	1	3

Table 16: Observed event yields in high-p_T (pT $>$ 20/10) dileptons passing the *simplified model* signal selections ($H_T > 200$ GeV, $\not{E}_T >$ 120GeV) compared to expectations from simulation alone, and from the data-driven methods. The *simulated backgrounds* contribution includes contributions from genuine same-sign lepton pairs (WZ, ZZ, leptons from same-sign W from single-, double-parton, and $t\bar{t}W$ production), as well as electrons from converted photons in $V\gamma$ production. Entries with zero contributing events are reported with an uncertainty corresponding to one event. This uncertainty is not added to the total MC contribution. Systematic uncertainties (the second uncertainty if present) are displayed only for the final combined type of background, no systematic uncertainty is added for estimates with zero entries. Systematic uncertainties are 100% correlated among the channels.

Source	ee	$\mu\mu$	eμ	all
$t\bar{t} \to \ell\ell X$	0.162 $\pm$ 0.162	0.000 $\pm$ 0.144	0.000 $\pm$ 0.144	0.162 $\pm$ 0.162
$t\bar{t} \to \ell(b \to \ell)X$	0.733 $\pm$ 0.382	1.005 $\pm$ 0.473	1.117 $\pm$ 0.476	2.855 $\pm$ 0.772
$t\bar{t} \to \ell(\not{b} \to \ell)X$	0.333 $\pm$ 0.267	0.000 $\pm$ 0.144	0.000 $\pm$ 0.144	0.333 $\pm$ 0.267
$t\bar{t}$ other	0.000 $\pm$ 0.144	0.000 $\pm$ 0.144	0.000 $\pm$ 0.144	0.000 $\pm$ 0.144
tW	0.024 $\pm$ 0.024	0.028 $\pm$ 0.020	0.004 $\pm$ 0.021	0.056 $\pm$ 0.031
t, t-channel	0.031 $\pm$ 0.022	0.047 $\pm$ 0.047	0.009 $\pm$ 0.042	0.087 $\pm$ 0.053
t, s-channel	0.007 $\pm$ 0.005	0.004 $\pm$ 0.004	0.004 $\pm$ 0.004	0.014 $\pm$ 0.007
W+jets	0.000 $\pm$ 2.039	0.000 $\pm$ 2.039	0.745 $\pm$ 2.039	0.745 $\pm$ 2.039
$Z \to ee$	0.000 $\pm$ 1.169	0.000 $\pm$ 1.169	0.000 $\pm$ 1.169	0.000 $\pm$ 1.169
$Z \to \mu\mu$	0.000 $\pm$ 1.169	0.000 $\pm$ 1.169	0.000 $\pm$ 1.169	0.000 $\pm$ 1.169
$Z \to \tau\tau$	0.000 $\pm$ 1.169	0.000 $\pm$ 1.169	0.000 $\pm$ 1.169	0.000 $\pm$ 1.169
WW	0.000 $\pm$ 0.040	0.000 $\pm$ 0.040	0.000 $\pm$ 0.040	0.000 $\pm$ 0.040
WZ	0.051 $\pm$ 0.023	0.081 $\pm$ 0.030	0.287 $\pm$ 0.057	0.418 $\pm$ 0.068
ZZ	0.006 $\pm$ 0.005	0.001 $\pm$ 0.001	0.005 $\pm$ 0.005	0.012 $\pm$ 0.007
Vγ	0.000 $\pm$ 0.210	0.000 $\pm$ 0.210	0.000 $\pm$ 0.210	0.000 $\pm$ 0.210
spW^+W^+	0.147 $\pm$ 0.013	0.219 $\pm$ 0.016	0.359 $\pm$ 0.021	0.725 $\pm$ 0.030
spW^-W^-	0.041 $\pm$ 0.004	0.059 $\pm$ 0.004	0.103 $\pm$ 0.006	0.204 $\pm$ 0.008
dp$W^\pm W^\pm$	0.000 $\pm$ 0.002	0.002 $\pm$ 0.002	0.002 $\pm$ 0.002	0.004 $\pm$ 0.003
$t\bar{t}W$	0.280 $\pm$ 0.010	0.453 $\pm$ 0.013	0.776 $\pm$ 0.017	1.509 $\pm$ 0.024
Total MC	1.813 $\pm$ 0.495	1.899 $\pm$ 0.477	3.410 $\pm$ 0.887	7.122 $\pm$ 1.122
LM6	0.952 $\pm$ 0.042	1.217 $\pm$ 0.048	2.037 $\pm$ 0.061	4.206 $\pm$ 0.088
Prompt-fake	1.86 $\pm$ 0.95	1.81 $\pm$ 0.87	3.05 $\pm$ 1.33	6.71 $\pm$ 1.70
Double-fake	0.00 $\pm$ 0.27	0.00 $\pm$ 0.26	0.13 $\pm$ 0.10	0.13 $\pm$ 0.10
Total with fakes	1.86 $\pm$ 0.78 $\pm$ 0.93	1.81 $\pm$ 0.70 $\pm$ 0.90	3.18 $\pm$ 1.32 $\pm$ 1.59	6.84 $\pm$ 1.69 $\pm$ 3.42
Charge misreconstruction	0.122 $\pm$ 0.019 $\pm$ 0.024	- $\pm$ -	0.153 $\pm$ 0.018 $\pm$ 0.031	0.275 $\pm$ 0.026 $\pm$ 0.055
Simulated backgrounds	0.525 $\pm$ 0.029 $\pm$ 0.262	0.815 $\pm$ 0.037 $\pm$ 0.408	1.531 $\pm$ 0.063 $\pm$ 0.766	2.871 $\pm$ 0.079 $\pm$ 1.436
All backgrounds	2.51 $\pm$ 0.78 $\pm$ 0.97	2.62 $\pm$ 0.70 $\pm$ 0.99	4.86 $\pm$ 1.32 $\pm$ 1.76	9.99 $\pm$ 1.69 $\pm$ 3.71
Data	3	2	2	7

Table 17: Observed event yields in high-p_T (pT $>$ 20/10) dileptons passing the *pMSSW/sneutrino* signal selections ($H_T > 80$ GeV, $\not{E}_T >$ 100 GeV) compared to expectations from simulation alone, and from the data-driven methods. The *simulated backgrounds* contribution includes contributions from genuine same-sign lepton pairs (WZ, ZZ, leptons from same-sign W from single-, double-parton, and $t\bar{t}W$ production), as well as electrons from converted photons in $V\gamma$ production. Entries with zero contributing events are reported with an uncertainty corresponding to one event. This uncertainty is not added to the total MC contribution. Systematic uncertainties (the second uncertainty if present) are displayed only for the final combined type of background, no systematic uncertainty is added for estimates with zero entries. Systematic uncertainties are 100% correlated among the channels.

Source	ee	$\mu\mu$	eμ	all
$t\bar{t} \to \ell\ell X$	0.595 ± 0.346	0.000 ± 0.144	0.231 ± 0.203	0.826 ± 0.401
$t\bar{t} \to \ell(b \to \ell)X$	2.223 ± 0.679	8.062 ± 1.289	7.331 ± 1.197	17.616 ± 1.885
$t\bar{t} \to \ell(\not{b} \to \ell)X$	1.405 ± 0.526	0.216 ± 0.216	0.763 ± 0.372	2.384 ± 0.679
$t\bar{t}$ other	0.000 ± 0.144	0.000 ± 0.144	0.000 ± 0.144	0.000 ± 0.144
tW	0.038 ± 0.038	0.387 ± 0.100	0.353 ± 0.103	0.778 ± 0.149
t, t-channel	0.078 ± 0.052	0.657 ± 0.183	0.789 ± 0.218	1.524 ± 0.290
t, s-channel	0.005 ± 0.005	0.014 ± 0.008	0.012 ± 0.007	0.031 ± 0.011
W+jets	0.000 ± 2.039	0.000 ± 2.039	3.027 ± 2.401	3.027 ± 2.401
$Z \to ee$	0.000 ± 1.169	0.000 ± 1.169	0.000 ± 1.169	0.000 ± 1.169
$Z \to \mu\mu$	0.000 ± 1.169	0.000 ± 1.169	0.000 ± 1.169	0.000 ± 1.169
$Z \to \tau\tau$	0.000 ± 1.169	0.000 ± 1.169	0.000 ± 1.169	0.000 ± 1.169
WW	0.000 ± 0.040	0.000 ± 0.040	0.000 ± 0.040	0.000 ± 0.040
WZ	0.131 ± 0.037	0.231 ± 0.053	0.409 ± 0.068	0.771 ± 0.093
ZZ	0.018 ± 0.009	0.021 ± 0.008	0.038 ± 0.012	0.076 ± 0.017
Vγ	0.372 ± 0.372	0.000 ± 0.210	0.000 ± 0.210	0.372 ± 0.372
spW^+W^+	0.299 ± 0.019	0.458 ± 0.023	0.761 ± 0.030	1.517 ± 0.043
spW^-W^-	0.086 ± 0.005	0.146 ± 0.007	0.223 ± 0.008	0.455 ± 0.012
dp$W^\pm W^\pm$	0.000 ± 0.002	0.002 ± 0.002	0.004 ± 0.003	0.006 ± 0.003
$t\bar{t}W$	0.544 ± 0.014	0.898 ± 0.019	1.466 ± 0.024	2.908 ± 0.033
Total MC	5.792 ± 1.001	11.091 ± 1.325	15.408 ± 2.728	32.291 ± 3.193
LM6	1.008 ± 0.043	1.509 ± 0.053	2.332 ± 0.065	4.849 ± 0.095
Prompt-fake	8.68 ± 2.22	11.84 ± 3.91	19.83 ± 3.48	40.35 ± 5.68
Double-fake	0.25 ± 0.23	7.31 ± 1.10	2.63 ± 0.63	10.19 ± 1.29
Total with fakes	8.93 ± 2.18 ± 4.46	19.15 ± 3.41 ± 9.57	22.46 ± 3.30 ± 11.23	50.54 ± 5.22 ± 25.27
Charge misreconstruction	0.657 ± 0.049 ± 0.131	- ± -	0.273 ± 0.025 ± 0.055	0.931 ± 0.055 ± 0.186
Simulated backgrounds	1.449 ± 0.375 ± 0.724	1.755 ± 0.062 ± 0.878	2.901 ± 0.079 ± 1.450	6.105 ± 0.388 ± 3.052
All backgrounds	11.04 ± 2.22 ± 4.52	20.90 ± 3.41 ± 9.61	25.63 ± 3.30 ± 11.32	57.57 ± 5.24 ± 25.45
Data	7	23	19	49

Table 18: Observed event yields in baseline low-p_T dileptons ($H_T > 200$ GeV, $\not{E}_T > 30$ GeV, lepton pT $> 10(5)$ GeV for electrons (muons)) compared to expectations from simulation alone, and from the data-driven methods. The *simulated backgrounds* contribution includes contributions from genuine same-sign lepton pairs (WZ, ZZ, leptons from same-sign W from single-, double-parton, and $t\bar{t}W$ production), as well as electrons from converted photons in $V\gamma$ production. Entries with zero contributing events are reported with an uncertainty corresponding to one event. This uncertainty is not added to the total MC contribution. Systematic uncertainties (the second uncertainty if present) are displayed only for the final combined type of background, no systematic uncertainty is added for estimates with zero entries. Systematic uncertainties are 100% correlated among the channels.

Source	ee	$\mu\mu$	eμ	all
$t\bar{t} \to \ell\ell X$	0.000 $\pm$ 0.144	0.000 $\pm$ 0.144	0.000 $\pm$ 0.144	0.000 $\pm$ 0.144
$t\bar{t} \to \ell(b \to \ell)X$	0.000 $\pm$ 0.144	0.031 $\pm$ 0.144	0.328 $\pm$ 0.243	0.358 $\pm$ 0.245
$t\bar{t} \to \ell(\not{b} \to \ell)X$	0.000 $\pm$ 0.144	0.000 $\pm$ 0.144	0.000 $\pm$ 0.144	0.000 $\pm$ 0.144
$t\bar{t}$ other	0.000 $\pm$ 0.144	0.000 $\pm$ 0.144	0.000 $\pm$ 0.144	0.000 $\pm$ 0.144
tW	0.000 $\pm$ 0.021	0.000 $\pm$ 0.021	0.000 $\pm$ 0.021	0.000 $\pm$ 0.021
t, t-channel	0.015 $\pm$ 0.042	0.000 $\pm$ 0.042	0.000 $\pm$ 0.042	0.015 $\pm$ 0.042
t, s-channel	0.000 $\pm$ 0.003	0.000 $\pm$ 0.003	0.000 $\pm$ 0.003	0.000 $\pm$ 0.003
W+jets	0.000 $\pm$ 2.039	0.000 $\pm$ 2.039	0.000 $\pm$ 2.039	0.000 $\pm$ 2.039
$Z \to ee$	0.000 $\pm$ 1.169	0.000 $\pm$ 1.169	0.000 $\pm$ 1.169	0.000 $\pm$ 1.169
$Z \to \mu\mu$	0.000 $\pm$ 1.169	0.000 $\pm$ 1.169	0.000 $\pm$ 1.169	0.000 $\pm$ 1.169
$Z \to \tau\tau$	0.000 $\pm$ 1.169	0.000 $\pm$ 1.169	0.000 $\pm$ 1.169	0.000 $\pm$ 1.169
WW	0.000 $\pm$ 0.040	0.000 $\pm$ 0.040	0.000 $\pm$ 0.040	0.000 $\pm$ 0.040
WZ	0.006 $\pm$ 0.006	0.000 $\pm$ 0.008	0.056 $\pm$ 0.026	0.062 $\pm$ 0.027
ZZ	0.000 $\pm$ 0.003	0.000 $\pm$ 0.003	0.000 $\pm$ 0.003	0.000 $\pm$ 0.003
Vγ	0.000 $\pm$ 0.210	0.000 $\pm$ 0.210	0.000 $\pm$ 0.210	0.000 $\pm$ 0.210
spW^+W^+	0.047 $\pm$ 0.008	0.076 $\pm$ 0.010	0.146 $\pm$ 0.013	0.269 $\pm$ 0.018
spW^-W^-	0.011 $\pm$ 0.002	0.018 $\pm$ 0.002	0.025 $\pm$ 0.003	0.055 $\pm$ 0.004
dp$W^\pm W^\pm$	0.000 $\pm$ 0.002	0.000 $\pm$ 0.002	0.000 $\pm$ 0.002	0.000 $\pm$ 0.002
$t\bar{t}W$	0.046 $\pm$ 0.004	0.089 $\pm$ 0.006	0.148 $\pm$ 0.008	0.283 $\pm$ 0.010
Total MC	0.126 $\pm$ 0.019	0.213 $\pm$ 0.033	0.703 $\pm$ 0.245	1.042 $\pm$ 0.248
LM6	0.819 $\pm$ 0.039	1.230 $\pm$ 0.048	1.861 $\pm$ 0.058	3.909 $\pm$ 0.085
Prompt-fake	0.31 $\pm$ 0.97	0.90 $\pm$ 0.65	0.31 $\pm$ 0.76	1.52 $\pm$ 0.80
Double-fake	0.00 $\pm$ 0.46	0.08 $\pm$ 0.08	0.00 $\pm$ 0.34	0.08 $\pm$ 0.08
Total with fakes	0.31 $\pm$ 0.32 $\pm$ 0.15	0.98 $\pm$ 0.64 $\pm$ 0.49	0.31 $\pm$ 0.32 $\pm$ 0.15	1.60 $\pm$ 0.79 $\pm$ 0.80
Charge misreconstruction	0.012 $\pm$ 0.006 $\pm$ 0.002	- $\pm$ -	0.014 $\pm$ 0.006 $\pm$ 0.003	0.026 $\pm$ 0.008 $\pm$ 0.005
Simulated backgrounds	0.111 $\pm$ 0.011 $\pm$ 0.055	0.183 $\pm$ 0.011 $\pm$ 0.091	0.375 $\pm$ 0.031 $\pm$ 0.187	0.669 $\pm$ 0.034 $\pm$ 0.334
All backgrounds	0.43 $\pm$ 0.32 $\pm$ 0.16	1.16 $\pm$ 0.64 $\pm$ 0.50	0.70 $\pm$ 0.33 $\pm$ 0.24	2.29 $\pm$ 0.79 $\pm$ 0.87
Data	0	1	0	1

Table 19: Observed event yields in low-p_T dileptons passing the *low-m_0* signal selections ($H_T > 400$ GeV, $\not{E}_T >$ 120 GeV) compared to expectations from simulation alone, and from the data-driven methods. The *simulated backgrounds* contribution includes contributions from genuine same-sign lepton pairs (WZ, ZZ, leptons from same-sign W from single-, double-parton, and $t\bar{t}W$ production), as well as electrons from converted photons in $V\gamma$ production. Entries with zero contributing events are reported with an uncertainty corresponding to one event. This uncertainty is not added to the total MC contribution. Systematic uncertainties (the second uncertainty if present) are displayed only for the final combined type of background, no systematic uncertainty is added for estimates with zero entries. Systematic uncertainties are 100% correlated among the channels.

Source	ee	$\mu\mu$	eμ	all
$t\bar{t} \to \ell\ell X$	0.000 $\pm$ 0.144	0.000 $\pm$ 0.144	0.000 $\pm$ 0.144	0.000 $\pm$ 0.144
$t\bar{t} \to \ell(b \to \ell)X$	0.255 $\pm$ 0.255	0.759 $\pm$ 0.381	1.098 $\pm$ 0.507	2.113 $\pm$ 0.683
$t\bar{t} \to \ell(\not{b} \to \ell)X$	0.255 $\pm$ 0.255	0.000 $\pm$ 0.144	0.247 $\pm$ 0.219	0.502 $\pm$ 0.336
$t\bar{t}$ other	0.000 $\pm$ 0.144	0.000 $\pm$ 0.144	0.000 $\pm$ 0.144	0.000 $\pm$ 0.144
tW	0.000 $\pm$ 0.021	0.024 $\pm$ 0.018	0.038 $\pm$ 0.038	0.062 $\pm$ 0.042
t, t-channel	0.015 $\pm$ 0.042	0.000 $\pm$ 0.042	0.032 $\pm$ 0.032	0.048 $\pm$ 0.036
t, s-channel	0.000 $\pm$ 0.003	0.000 $\pm$ 0.003	0.000 $\pm$ 0.003	0.000 $\pm$ 0.003
W+jets	0.000 $\pm$ 2.039	0.000 $\pm$ 2.039	0.000 $\pm$ 2.039	0.000 $\pm$ 2.039
$Z \to ee$	0.000 $\pm$ 1.169	0.000 $\pm$ 1.169	0.000 $\pm$ 1.169	0.000 $\pm$ 1.169
$Z \to \mu\mu$	0.000 $\pm$ 1.169	0.000 $\pm$ 1.169	0.000 $\pm$ 1.169	0.000 $\pm$ 1.169
$Z \to \tau\tau$	0.000 $\pm$ 1.169	0.000 $\pm$ 1.169	0.000 $\pm$ 1.169	0.000 $\pm$ 1.169
WW	0.000 $\pm$ 0.040	0.000 $\pm$ 0.040	0.000 $\pm$ 0.040	0.000 $\pm$ 0.040
WZ	0.013 $\pm$ 0.009	0.021 $\pm$ 0.016	0.062 $\pm$ 0.027	0.096 $\pm$ 0.032
ZZ	0.000 $\pm$ 0.003	0.001 $\pm$ 0.001	0.000 $\pm$ 0.003	0.001 $\pm$ 0.001
Vγ	0.000 $\pm$ 0.210	0.000 $\pm$ 0.210	0.000 $\pm$ 0.210	0.000 $\pm$ 0.210
spW^+W^+	0.102 $\pm$ 0.011	0.146 $\pm$ 0.013	0.279 $\pm$ 0.018	0.527 $\pm$ 0.025
spW^-W^-	0.026 $\pm$ 0.003	0.038 $\pm$ 0.003	0.061 $\pm$ 0.004	0.125 $\pm$ 0.006
dp$W^\pm W^\pm$	0.000 $\pm$ 0.002	0.000 $\pm$ 0.002	0.002 $\pm$ 0.002	0.002 $\pm$ 0.002
$t\bar{t}W$	0.114 $\pm$ 0.007	0.186 $\pm$ 0.008	0.317 $\pm$ 0.011	0.617 $\pm$ 0.015
Total MC	0.782 $\pm$ 0.362	1.175 $\pm$ 0.382	2.137 $\pm$ 0.555	4.094 $\pm$ 0.765
LM6	0.878 $\pm$ 0.040	1.315 $\pm$ 0.050	2.036 $\pm$ 0.061	4.229 $\pm$ 0.088
Prompt-fake	1.03 $\pm$ 1.05	1.97 $\pm$ 1.00	0.61 $\pm$ 0.49	3.61 $\pm$ 1.22
Double-fake	0.00 $\pm$ 0.46	0.17 $\pm$ 0.12	0.08 $\pm$ 0.08	0.25 $\pm$ 0.15
Total with fakes	1.03 $\pm$ 0.50 $\pm$ 0.51	2.15 $\pm$ 0.98 $\pm$ 1.07	0.68 $\pm$ 0.47 $\pm$ 0.34	3.86 $\pm$ 1.20 $\pm$ 1.93
Charge misreconstruction	0.057 $\pm$ 0.015 $\pm$ 0.011	- $\pm$ -	0.030 $\pm$ 0.008 $\pm$ 0.006	0.086 $\pm$ 0.017 $\pm$ 0.017
Simulated backgrounds	0.255 $\pm$ 0.016 $\pm$ 0.128	0.392 $\pm$ 0.023 $\pm$ 0.196	0.721 $\pm$ 0.035 $\pm$ 0.361	1.369 $\pm$ 0.044 $\pm$ 0.685
All backgrounds	1.34 $\pm$ 0.50 $\pm$ 0.53	2.54 $\pm$ 0.98 $\pm$ 1.09	1.43 $\pm$ 0.47 $\pm$ 0.50	5.31 $\pm$ 1.20 $\pm$ 2.05
Data	1	4	2	7

Table 20: Observed event yields in low-p_T dileptons passing the *high-*m_0 signal selections ($H_T > 400$ GeV, $\not{E}_T > 50$ GeV) compared to expectations from simulation alone, and from the data-driven methods. The *simulated backgrounds* contribution includes contributions from genuine same-sign lepton pairs (WZ, ZZ, leptons from same-sign W from single-, double-parton, and $t\bar{t}W$ production), as well as electrons from converted photons in $V\gamma$ production. Entries with zero contributing events are reported with an uncertainty corresponding to one event. This uncertainty is not added to the total MC contribution. Systematic uncertainties (the second uncertainty if present) are displayed only for the final combined type of background, no systematic uncertainty is added for estimates with zero entries. Systematic uncertainties are 100% correlated among the channels.

Source	ee	$\mu\mu$	eμ	all
$t\bar{t} \to \ell\ell X$	0.000 ± 0.144	0.000 ± 0.144	0.000 ± 0.144	0.000 ± 0.144
$t\bar{t} \to \ell(b \to \ell)X$	0.000 ± 0.144	1.345 ± 0.573	1.228 ± 0.489	2.572 ± 0.753
$t\bar{t} \to \ell(\not{b} \to \ell)X$	0.000 ± 0.144	0.000 ± 0.144	0.000 ± 0.144	0.000 ± 0.144
$t\bar{t}$ other	0.000 ± 0.144	0.000 ± 0.144	0.000 ± 0.144	0.000 ± 0.144
tW	0.000 ± 0.021	0.032 ± 0.020	0.000 ± 0.021	0.032 ± 0.020
t, t-channel	0.031 ± 0.022	0.047 ± 0.047	0.041 ± 0.034	0.119 ± 0.062
t, s-channel	0.000 ± 0.003	0.000 ± 0.003	0.000 ± 0.003	0.000 ± 0.003
W+jets	0.000 ± 2.039	0.000 ± 2.039	0.745 ± 2.039	0.745 ± 2.039
$Z \to ee$	0.000 ± 1.169	0.000 ± 1.169	0.000 ± 1.169	0.000 ± 1.169
$Z \to \mu\mu$	0.000 ± 1.169	0.000 ± 1.169	0.000 ± 1.169	0.000 ± 1.169
$Z \to \tau\tau$	0.000 ± 1.169	0.000 ± 1.169	0.000 ± 1.169	0.000 ± 1.169
WW	0.000 ± 0.040	0.000 ± 0.040	0.000 ± 0.040	0.000 ± 0.040
WZ	0.035 ± 0.017	0.035 ± 0.020	0.129 ± 0.039	0.199 ± 0.047
ZZ	0.005 ± 0.005	0.000 ± 0.003	0.000 ± 0.003	0.005 ± 0.005
Vγ	0.000 ± 0.210	0.000 ± 0.210	0.000 ± 0.210	0.000 ± 0.210
spW^+W^+	0.092 ± 0.010	0.148 ± 0.013	0.248 ± 0.017	0.488 ± 0.024
spW^-W^-	0.024 ± 0.003	0.044 ± 0.004	0.060 ± 0.004	0.128 ± 0.006
dp$W^\pm W^\pm$	0.000 ± 0.002	0.002 ± 0.002	0.000 ± 0.002	0.002 ± 0.002
$t\bar{t}W$	0.150 ± 0.008	0.269 ± 0.010	0.437 ± 0.013	0.856 ± 0.018
Total MC	0.336 ± 0.031	1.922 ± 0.576	2.889 ± 0.893	5.146 ± 1.063
LM6	0.915 ± 0.041	1.367 ± 0.051	2.077 ± 0.062	4.359 ± 0.090
Prompt-fake	1.15 ± 1.10	2.17 ± 1.05	1.01 ± 0.75	4.33 ± 1.42
Double-fake	0.00 ± 0.46	0.28 ± 0.17	0.20 ± 0.15	0.49 ± 0.23
Total with fakes	1.15 ± 0.61 ± 0.58	2.45 ± 1.01 ± 1.23	1.22 ± 0.70 ± 0.61	4.82 ± 1.37 ± 2.41
Charge misreconstruction	0.032 ± 0.009 ± 0.006	- ± -	0.050 ± 0.010 ± 0.010	0.083 ± 0.014 ± 0.017
Simulated backgrounds	0.305 ± 0.022 ± 0.153	0.498 ± 0.027 ± 0.249	0.874 ± 0.045 ± 0.437	1.677 ± 0.057 ± 0.839
All backgrounds	1.49 ± 0.61 ± 0.60	2.95 ± 1.01 ± 1.25	2.14 ± 0.70 ± 0.75	6.58 ± 1.37 ± 2.55
Data	0	4	2	6

Table 21: Observed event yields in low-p_T dileptons passing the *simplified model* signal selections ($H_T > 200$ GeV, $\not{E}_T > 120$ GeV) compared to expectations from simulation alone, and from the data-driven methods. The *simulated backgrounds* contribution includes contributions from genuine same-sign lepton pairs (WZ, ZZ, leptons from same-sign W from single-, double-parton, and $t\bar{t}W$ production), as well as electrons from converted photons in $V\gamma$ production. Entries with zero contributing events are reported with an uncertainty corresponding to one event. This uncertainty is not added to the total MC contribution. Systematic uncertainties (the second uncertainty if present) are displayed only for the final combined type of background, no systematic uncertainty is added for estimates with zero entries. Systematic uncertainties are 100% correlated among the channels.

8.1 Summary of results

To summarize: we see no evidence for an anomalous rate of same sign isolated dilepton events either at the preselection (baseline) level or at high $\not{E}_T$ or high H_T. This observation can be interpreted as upper limits on potential new physics models.

Based on the results reported in Table 14 the high-p_T dilepton region wtih $H_T > 400$ GeV and $\not{E}_T > 120$ GeV, we can set an upper limit on the number of signal events of 3.1, which is based on the Bayesian calculation with uniform signal strength and log-normal uncertainties on the efficiency and background estimates used as nuisance parameters. The uncertainty on the efficiency here is 14%, as will be described in detail later in Section 9.4. This upper limit of 3.1 events at 95% can be compared to 3.6 (4.6) events expected in the reference LM6 model point at LO (NLO).

9 Systematics

Systematic uncertainties arise from uncertainties on event selections expected in simulation compared to the actual performance of the detector, from uncertainties on the fraction of events passing all selections due to uncertainties on signal production at the origin (prior to detector effects), and from the absolute normalization of the total number of expected events due to an uncertainty on the total integrated luminosity (currently recommended to be 6% for the 2011 data).

For the measurement of, or search for, a known and well defined signal, calculating all of these is straightforward. However, in our case, we are attempting to present our search result in as "model independent" a way as possible, i.e. with as little recourse to a well defined signal as possible. This makes assigning the first two types of systematic errors mentioned above a little less obvious.

We thus chose two "representative models" for our signal, and evaluate some of the systematics with reference to those two signal models. Those two signal models are "same sign top production" and the SUSY reference point LM6. For same sign top production, we calculate systematics on the efficiency and acceptance only for the baseline selections, which are similar to those in the corresponding opposite sign $t\bar{t}$ analysis [1], results obtained in [20] are reused in this case.

The following systematic uncertainties are thus considered:

- The uncertainty on event selection efficiency differences in simulation compared to data includes the following
  - Uncertainty on the lepton selection efficiency, as discussed in Section 5.4. We then assign a systematic for possible differences in the isolation efficiency due to event environment between the Z sample for which we do tag-and-probe, and the $t\bar{t}$ or LM6 samples, which we use as generic "models" for our search regions.
  - Uncertainty on the jet and missing energy selection is discussed in Section 9.2. It is estimated by the calorimeter energy in MC appropriately.
  - The uncertainties on the remaining selections (primary vertex, event cleaning, etc.) are negligible compared to the ones mentioned above as the corresponding efficiencies are essentially 100%.
- The uncertainty on the fraction of events produced at the origin is from theoretical uncertainties on event modeling. Based on the following, we assign a 2% systematics due to these kinds of uncertainties. These results are taken verbatim from our previous study, as there are no changes in the underlying physics.
  - Systematic variations of ISR/FSR. We take 1% based on a study for the $t\bar{t}$ cross section measurement presented in [1].
  - PDF uncertainties on the efficiency were found to be less than 1% for the $t\bar{t}$ cross section measurement presented in [1]. Applying an analogous procedure to an LM0 MC sample gives a relative uncertainty on the acceptance of approximately 1.5%, we use the same value for the LM6 reference model point. Reweighting the central value of the acceptance using the CTEQ66 PDFs with maximal and minimal α_s values yielded a change in acceptance of less than 0.2%.
- Uncertainties on the background estimates contribute to the systematic uncertainty of the cross section measurement. Those were already described in Section 8. In summary:

- Systematic on the fake lepton background estimate is 50% .
- Systematic on charge flip background estimate is 20% .
- Systematic error on the residual background estimated using MC is 50% .

Table 23 presents a summary of all systematic uncertainties.

9.1 Systematic uncertainty of lepton selection

The MC-to-data scale factors and their uncertainties are presented in Section 5.4. As both of these are P_T dependent, we need to pick some model to apply them to. We use LM6 and opposite sign $t\bar{t}$ as our reference models. The uncertainty on modeling of the isolation in signal events is estimated separately based on a comparison of the isolation efficiency for the reference LM6 model and Z events where we can confirm the isolation performance on data. We assume that the simulation reproduces the isolation efficiency for signal events well; the difference between the isolation efficiency per lepton in Z and LM6 changes from approximately 10% at higer momenta to about 20% at lower momenta. The effect is smaller for $t\bar{t}$ A somewhat arbitrary value of 10% per dilepton, used in the previous analysis, is applied here to account for the uncertainty of the isolation requirement.

Contributions to the systematic uncertainty due to lepton selections are summarized in Table 22. Note that the HT triggers have an additional 5% systematic uncertainty for HT between 200 and 300 GeV, which is further ignored. The uncertainties on electron and muon reconstruction efficiencies were below 2% in 2010 data [1], in agreement with estimates presented in VBTF, and muon-POG groups. We keep 2% for all lepton types. The trigger systematics is discussed in Section 4, an uncertainty of 4% will cover the trigger systematics sufficiently well for all triggers considered, except for the muon triggers for the momentum range of 5–10 GeV, where the uncertainty is 5% per muon in agreement with [3]. It is still much smaller than the dominant uncertainty due to the isolation efficiency, thus higher precision estimates are not going to change the final result.

Table 22: Summary of contributions to the lepton selection systematic uncertainty estimated for dileptons from $t\bar{t}$. The values displayed are fractional uncertainties. The values in parentheses are for momenta below 20 GeV for electrons and below 15 GeVfor muons. The value for all is simply copied from the $e\mu$.

Source	ee	$\mu\mu$	$e\mu$	All
Trigger	4%	4(10)%	4(5)%	4%
Reconstruction	2%	2%	2%	2%
Identification and isolation	3(10)%	2(10)%	2(10)%	2(10)%
Simulation LM6 vs Z	10%	10%	10%	10%
Combined	11(15)%	11(17)%	11(15)%	11(15)%

9.2 Jet and MET selection uncertainty

We vary jet energy in simulation by $\pm 7.5\%$ simultaneously with $\pm 7.5\%$ variation in the missing transverse energy excluding the two candidate same sign leptons to test the sensitivity of the jet and missing energy selections to the uncertainty in the energy scale. This uncertainty is estimated as an average for 40 GeV jets with $|\eta| < 2.5$, as used in the analysis. It arises from the following sources:

- Fall10 JES uncertainty of 1.3-2.5% for PFJets at $p_T > 30$ GeV and $|\eta| < 3.0$ [22];
- 2% for jets with $|\eta| < 1.5$ and 6% for jets in $1.5 < |\eta| < 3.0$ [16];
- 5% due to pileup for a jet with $p_T = 40$ GeV in events with 10 vertices, based on the average uncertainty per vertex of $(0.2\text{ GeV})/p_T$ [19].

The variations in the number of events passing full event selections are used as an estimate on the jet and missing energy scale systematic uncertainty.

The results of these variations are 6% for the same-sign top signal in the baseline selection region with hihg-p_T dileptons. The result for the LM6 point is approximately 3% for the selection with $H_T > 400$ GeV and $\not\!\!E_T > 120$ GeV; it is smaller on all less restrictive selections. To keep things simple, we assign a $\pm 5\%$ systematics due to the JES uncertainty for all regions.

9.3 Background estimates

Backgrounds considered in this analysis are estimated partly using data-driven methods and partly from simulation. We assign a 50% on the total number of background events estimated from Monte Carlo. The uncertainty on the fake lepton predictions are 50% (ignoring the larger uncertainty on the small double-fake prediction). The uncertainty on the rate of events with electrons with misreconstructed charge is 20%.

9.4 Summary of systematic uncertainties

Systematic uncertainties are summarized in Table 23.

Table 23: Summary of systematic uncertainties on the signal selection and expectation. Reported values are fractional, relative to the total cross section. The values in parentheses are for the low-p_T dileptons. The value for all is simply copied from the $e\mu$.

Source	ee	$\mu\mu$	$e\mu$	all
Lepton selection	11(15)%	11(17)%	11(15)%	11(15)%
Energy scale	5%	5%	5%	5%
ISR/FSR and PDF	2%	2%	2%	2%
Total without luminosity	12(16)%	12(18)%	12(16)	12(16)%
Integrated luminosity	6%	6%	6%	6%
Total	14(17)%	14(19)%	14(17)%	14(17)%

10 Summary

We performed an analysis of same-sign dilepton events in 2011 data sample of 976 pb^{-1}. The observed number of events is in agreement with background expectations. Based on this observation we can set limits on new physics models. As an example, we exclude LM6 CMSSM model point.

References

[1] http://arxiv.org/abs/1105.5661; D. Barge *et al.* AN-CMS2010/410; CMS PAS **TOP-11-002**.

[2] D. Barge *et al.*, AN-CMS2010/257.

[3] D. Acosta *et al.*, AN-CMS2011/184.

[4] `https://twiki.cern.ch/twiki/bin/viewauth/CMS/SameSignDilepton2011`

[5] `https://twiki.cern.ch/twiki/bin/viewauth/CMS/SUSYMCRequirements0911`

[6] https://twiki.cern.ch/twiki/bin/viewauth/CMS/SimpleCutBasedEleID

[7] PAS EWK-10-002.

[8] D. Barge *et al.*, AN-CMS2009/159.

[9] D. Barge *et al.*, AN-CMS2009/138.

[10] D. Barge *et al.*, AN-CMS2010/077.

[11] W. Andrews *et al.*, AN-2011/155.

[12] https://twiki.cern.ch/twiki/bin/view/CMS/StandardModelCrossSections

[13] W. Andrews *et al.*, AN-CMS2010/274.

[14] J. Conway, `http://www-cdf.fnal.gov/physics/statistics/code/bayes.f`.

[15] Details on this grid will be documented in AN-CMS2010/372 .

[16] `https://twiki.cern.ch/twiki/bin/view/CMS/JECDataMC`

[17] T.Han, Private Communications.

[18] S. Harper, private communication (relayed to us by M. Chiorboli.).

[19] M. Voutilainen *et al.* AN-2011/105.

[20] S. Chatrchyan *et al.* [CMS Collaboration], arXiv:1104.3168 [hep-ex].

[21] S. Chatrchyan *et al.* [CMS Collaboration], CMS Physics Analysis Summary **JME-10-009**.

[22] S. Chatrchyan *et al.* [CMS Collaboration], CMS Physics Analysis Summary **JME-10-011**.

[23] `https://twiki.cern.ch/twiki/bin/view/Sandbox/SameSignSneutrino2010`

A Log of Changes in the Note

A.1 Version 3 (2 was in error) in iCMS

- Added systematic uncertainties to the tables
- Fix the combined systematics table (forgot to propagate the lepton efficiencies).
- update the electron efficiency table and accompanying text after a fix to the selections.

A.2 Version 4 in iCMS

- Scale factor for charge flips introduced and explained
- Systematics for JES is changed to 7.5% based on available sources.

This was mistakenly mentioned as version 3 before.

A.3 Version 5 in iCMS

- Update all data yields to 976 pb^{-1}.
- Update tables with fake rates, using 882 pb^{-1}.
- Add event selection model curves and fits
- Updated Zee test for flip rates
- Added clarifications on systematics, cleaned up a bit, updated to LM6.
- Added a statment on exclusion of LM6.

B Contributions still missing in this note

To be completed in time for approval, sorted roughly in the order of importance.

1. Produce upper limits for the number of signal events (after all cuts). NB: for the PAS this was produced using our numbers by R. Remington (UFL).

To be completed in time for approval or whenever

- Revisit/update the isolation efficiency modeling systematics, esp for lower p_T, where we are cutting tighter now.
- Compute limits on reference models (mSUGRA)
- Compute limits on reference models (snutrino/pMSSM)
- Compute *model-independent* limits
- Update the $t\bar{t}$ closure tests with current selections; it makes sense to stick to the looser cuts for the W+jets tests due to stats.